THE EFFECTS OF ERROR CORRECTING CODES ON MIMO-OFDM SYSTEM USING OSTBC

GAMAL MAHMUD ALAUSTA

DECEMBER 2020

THE EFFECTS OF ERROR CORRECTING CODES ON MIMO-OFDM SYSTEM USING OSTBC

A THESIS SUBMITTED TO
THE GRADUATE SCHOOL OF NATURAL AND APPLIED
SCIENCES OF
ÇANKAYA UNIVERSITY

BY
GAMAL MAHMUD ALAUSTA

IN PARTIAL FULFILLMENT OF THE REQUIREMENTS FOR THE
DEGREE OF
DOCTORA OF PHILOSOPHY
IN
THE DEPARTMENT OF
ELECTRONIC AND COMMUNICATION ENGINEERING

DECEMBER 2020

ABSTRACT

THE EFFECTS OF ERROR CORRECTING CODES ON MIMO-OFDM SYSTEM USING OSTBC

GAMAL MAHMUD ALAUSTA
Ph.D., Department of Electronic and Communication Engineering
Supervisor: Prof. Dr. Halil Tanyer EYYUBOĞLU

DECEMBER 2020, 96 pages

The objective of this thesis is to study whether the combination of Orthogonal Space-Time Block Coding (OSTBC) for Multiple-Input-Multiple-Output (MIMO) and Orthogonal Frequency Division Multiplexing (OFDM) technologies in wireless communication systems would significantly improve the transmission reliability over multi-path MIMO fading channels. A MIMO system takes its benefits from spatial diversity, which is obtained from spatially separated antennas in a dense multipath scattering environment. In order to use the additional antennas for spatial diversity, the MIMO method implements space-time block coding. There are different types of Space-Time Coding techniques, such as Alamouti Space Time Coding, Orthogonal Space-Time Coding, Quasi Orthogonal Space Time Coding, etc. The Orthogonal Space-Time Coding technique is preferable over other techniques because it provides more reliable transmission than other Space-Time Coding techniques by utilizing the same number of transmitting and receiving antennas. OFDM system is an excellent way to utilize the spectrum. In contrast to serial communication systems, OFDM is a type of parallel data transmission that promises a lower reduction in service quality with a higher data rate. In OFDM, a single channel on adjacent frequencies uses multiple sub-carriers. The MIMO (OSTBC)-OFDM combination system is currently

accepted for modern mobile wireless communication schemes as one of the most competitive technologies. In this thesis, an OSTBC configuration is proposed for MIMO-OFDM systems in 1 × 1, 2 × 2, 3 × 3 and 4 × 4 antenna configurations. In this work, analyses of modulations such as QPSK, 16-QAM and 64-QAM on the MIMO (OSTBC)-OFDM system are presented and for the analysis, Rician and Rayleigh channels are used. Their effects are studied in detail on the bit error rate for high data rates. A comparative study shows that the performance of MIMO-OFDM using OSTBC with different types of modulation improves for high order antenna configurations for channel conditions and a given data rate. Such a performance improvement inevitably leads to a lower bit error rate (BER).

Keywords: MIMO, OFDM, OSTBC, Rayleigh fading channel, Rician fading channel, BER.

ÖZ

OSTBC KULLANARAK MIMO-OFDM SİSTEMİ ÜZERİNDEKİ HATA DÜZELTME KODLARININ ETKİLERİ

GAMAL MAHMUD ALAUSTA
Doktora, Elektronik ve Haberleşme Mühendisliği Anabilim Dalı
Tez Yöneticisi: Prof. Dr. Halil Tanyer EYYUBOĞLU
Aralik 2020, 96 sayfa

Bu tezin amacı, kablosuz iletişim sistemlerinde Çoklu Giriş-Çoklu Çıkış (MIMO) ve Ortogonal Frekans Bölmeli Çoğullama (OFDM) teknolojileri için Ortogonal Uzay-Zaman Blok Kodlama (OSTBC) kombinasyonunun çok yollu MIMO sönümleme kanalları üzerinden yapılan iletişimin güvenilirliğini önemli ölçüde iyileştirip iyileştirmediğini araştırmaktır. Bir MIMO sistemi, yoğun birçok yollu saçılma ortamında uzaysal olarak ayrılmış antenlerden elde edilen uzaysal çeşitlilikten yararlanır. Uzaysal çeşitlilik açısından ek antenleri kullanmak için, MIMO yöntemi uzay-zaman blok kodlamasını uygular. Alamouti Uzay Zaman Kodlaması, Ortogonal Uzay-Zaman Kodlaması, Yarı Ortogonal Uzay Zaman Kodlaması ve benzerleri gibi farklı Uzay-Zaman Kodlama teknikleri vardır. Ortogonal Uzay-Zaman Kodlama tekniği aynı sayıda verici ve alıcı anteni kullanarak diğer Uzay Zaman Kodlaması tekniklerinden daha güvenilir iletim sağladığı için diğer tekniklere göre tercih edilir. OFDM sistemi, spektrumu kullanmanın mükemmel bir yoludur. Seri iletişim sistemlerinin aksine OFDM, daha yüksek bir veri hızı ile hizmet kalitesinde daha düşük bir azalma öngören paralel bir veri aktarım çeşididir. OFDM'de, bitişik frekanslardaki tek kanal, birden çok alt taşıyıcı kullanır. MIMO (OSTBC) OFDM kombinasyon sistemi şu anda modern mobil kablosuz iletişim şemaları için en rekabetçi teknolojilerden biri olarak kabul edilmektedir. Bu tezde, 1 × 1, 2 × 2, 3 × 3

ve 4 × 4 anten konfigürasyonlarında MIMO OFDM sistemleri için bir OSTBC konfigürasyonu önerilmiştir. Bu çalışmada MIMO (OSTBC) OFDM sistemi üzerinde QPSK, 16 QAM ve 64 QAM gibi modülasyonların analizleri sunulmuş ve analiz için Rician ve Rayleigh kanalları kullanılmıştır. Etkileri, yüksek veri hızları için bit hata oranı konusu ile ilgili olarak ayrıntılı bir biçimde incelenmiştir. Karşılaştırmalı bir çalışma, farklı modülasyon türleri ile OSTBC kullanan MIMO-OFDM'nin performansının, kanal koşulları ve belirli bir veri hızı için yüksek sıralı anten konfigürasyonları için iyileştiğini göstermektedir. Böyle bir performans kaçınılmaz olarak daha düşük bir bit hata oranına (BER) yol açmaktadır.

Anahtar Kelimeler: MIMO, OFDM, OSTBC, Rayleigh sönümleme kanalı, Rician sönümleme kanalı, BER.

ACKNOWLEDGEMENTS

I would like to prompt my sincere appreciation to Prof. Dr. Halil Tanyer EYYUBOĞLU for his supervision, suggestions, special guidance, and encouragement through the development of this thesis.

I would like to thank the Ministry of Higher Education in Libya for its financial support. My achievements would not have been possible without their constant support and encouragement.

I give thanks to my committee, Prof. Dr. Halil Tanyer EYYUBOĞLU, Assoc. Prof. Dr. Özgür Tolga PUSATLI, Assoc. Prof. Dr. Orhan GAZİ, Asst. Prof. Dr Fatih Korkmaz and Assoc. Prof. Dr. Hüsnü Deniz BAŞDEMİR .

Sincere thanks to my family for their patience, understanding, and love. My achievements would not have been possible without their constant encouragement and support.

Finally, I express my grateful feelings to my friends in Libya and Turkey.

TABLE OF CONTENTS

LIST OF FIGURES

LIST OF TABLES

LIST OF ABBREVIATIONS

2G	2^{nd} Generation
3GPP	3^{th} Generation Partnership Project
4G	4^{th} Generation
5G	5^{th} Generation
ADC	Analog to Digital Conversion
ADSL	Asymmetric Digital Subscriber Line
AWGN	Additive White Gaussian Noise
BER	Bit Error Rate
BPSK	Binary Phase Shift Keying
BCH	The Bose, Chaudhuri, and Hocquenghem
BW	Band Width
CDMA	Code Division Multiple Access
CP	Cyclic Prefix
CSI	Channel State Information
CSI	Channel State Information
DAC	Digital to Analog Conversion
DAB	Digital Audio Broadcasting
DFT	Discrete Fourier Transform
DVB	Digital Video Broadcasting
DVB-T	Digital Video Broadcasting Terrestrial
DSL	Digital Subscriber Line
DSRC	Dedicated Short Range Communications
ETSI	European Telecommunications Standard Institute
FDD	Frequency Division Duplex
FDM	Frequency Division Multiplexing
FEC	Forward Error Correction

FFT	Fast Fourier transform
HSUPA	High-Speed Uplink Packet Access
ICI	InterCarrier Interference
IDFT	Inverse Discrete Fourier Transform
IFFT	Inverse Fast Fourier transform
IP	Internet Protocol
ISI	InterSymbol Interference
LAN	Local Area Network
LOS	Line of Sight
LFRS	Linear Feedback Shift Register
LSB	Least Significant Byte
LTE	Long Term Evolution
LTE-A	Long Term Evolution –Advanced
MAC	Medium Access Control
MCM	Multi-Carrier Modulation
MAN	Metropolitan area network
MIMO	Multiple Input Multiple Output
MISO	Multiple Input Single Output
MSB	Most Significant Byte
M-QAM	Mary Quadrature Amplitude Modulation
NLOS	Non Line of Sight
OFDM	Orthogonal Frequency Division Multiplexing
OFDMA	Orthogonal Frequency Division Multiple Access
OSTBC	Orthogonal Space Time Block Code
PAPR	Peak to Average Power Ratio
PRBS	Pseudo Random Binary Sequence
PLCs	power line communications
QAM	Quadrature amplitude modulation
QoS	Quality of Services

QPSK	Quadrature Phase-Shift Keying
SISO	Signal Input Signal Output
SIMO	Single Input Multiple Output
SNR	Signal to Noise Ratio
SINR	Signal to Noise Plus Interference Ratio
STBC	Space Time Block Code
STD	Spatial Transmit Diversity
STTC	Space Time Trellis Code
SVD	Singular Value Decomposition
TDD	Time Division Duplex
UMTS	Universal Mobile Telecommunication System
VoIP	Voice over IP
WLAN	Wireless Local Area Network
WT	Wavelet Transform
WiMAX	Worldwide Interoperability for Microwave Access
ZF	Zero Forcing

CHAPTER 1

INTRODUCTION

1.1 Overview

Wireless systems, the most significant communication systems in recent times have been growing steadily. Digital communication systems have succeeded in wireless communication systems for reasons associated with cost, bandwidth, flexibility, etc. For improved quality of service (QoS), different channel coding, multiple access schemes, data rates, bit error ratio (BER) and reliability throughput have been investigated by researchers for their advantages in design considerations. Forthcoming wireless communication networks are expected to include widespread access with higher speeds and higher reliability. In cellular networks, there has been a transition from Universal Mobile Telecommunication Systems (UMTSs) to Long Term Evolution (LTE) for enhanced data-rates and reliability and expanded coverage areas. Similarly, there has been an evolution in wireless local area networks (WLAN) from IEEE 802.11n to IEEE 802.11ac and IEEE 802.11ad to satisfy the increasing demand for high-speed wireless applications. Recently, an enhanced FDM technology, Orthogonal Frequency Division Multiplexing (OFDM) and Orthogonal Frequency Division Multiplexing Access (OFDMA) have dominated the market as the air interface protocol for wideband systems, including those employing multi-antenna technology. The most common examples include wireless reliability (Wi-Fi), worldwide interoperability for microwave access (WiMAX), digital audio/video broadcasting (DAB/DVB), and LTE. The OFDM scheme has been preferred because it is more robust than frequency selective transmissions. OFDM is efficiently applied using the Fast Fourier Transform (FFT), which enables the use of frequency domain equalization, an additional scheme for reducing multipath. Thus, mobile base stations are expected to offer easy services irrespective of the mobile speed. Modern broadband technologies must be able to provide excellent QoS at high speed.

Moreover, modern telecommunication systems use multiple antennas. To achieve a rich and seamless QoS, MIMO designs must yield an excellent diversity gain and spatial diversity index.

1.2 OFDM

OFDM is a common technique for high data rate wireless transmission methods [1]. OFDM has been adopted in several wireless standards, such as digital audio broadcasting (DAB), digital video broadcasting (DVB), the IEEE 802.11e [2] LAN standard, and the IEEE 802.16a [3] MAN standard. Likewise, OFDM is used for dedicated short-range communications (DSRC) on the roadside for car communications, and it can be a possible candidate for the fourth-generation (4G) mobile wireless project. OFDM changes a frequency-selective channel into a parallel group of the frequency with flat sub-channels. The sub-carriers have the smallest required frequency separation amount to keep orthogonality of their response time-domain waveforms and yet the signal spectra response to the various sub-carriers overlap in frequency. Thus, the available bandwidth can be used at the highest efficiency. If the transmitter has channel information, then the OFDM transmitter will adjust its signaling strategy to match the channel. Since OFDM uses a large group of closely spaced sub-channels, these adaptive plans can approximate the ideal water-pouring capacity of a frequency-selective channel. This is attained in practice by using methods of adaptive bit loading, where the signal constellations of various sizes are transmitted over the sub-carriers. OFDM is a technique for block modulation where a block of N information symbols is transmitted in parallel with N sub-carriers. The duration of an OFDM symbol is N times greater than a single carrier scheme. An OFDM modulator can be used as an IDFT on a block of N data symbols followed by an ADC. To decrease the ISI effects caused by the spread of channel time, each block of IDFT coefficients is preceded by a guard interval or a CP consisting of G samples. This means that the length of the CP is at least equivalent to the length of the channel. As a result, the effects of the ISI are easily and eliminated. In addition, this method provides an opportunity to the receiver to use a very fast signal which processes transforms such as FFT for OFDM applications [4]. Similar methods can also be used in single carrier systems by following all transmitted data blocks of length N by a CP, while using frequency-

domain equalization at the receiver. OFDM schemes are interesting because of the manner in which they handle ISI, which is usually put in by frequency selective multipath fading in a wireless communication environment. Every sub-carrier is moderated at the minimum symbol rate which allows the symbols to be longer than the duration of channel impulse response; therefore, ISI is decreased. In addition, if a guard interval is introduced between consecutive OFDM symbols, it can decrease the impacts of ISI. The multipath delay must be shorter than the guard interval. Although every sub-carrier activates at the minimum data rate, in total a maximum data rate can be achieved by using many sub-carriers. ISI has either a small or no impact on the OFDM schemes; therefore, there is no need for an equalizer from the receiver side. OFDM has many benefits compared to other transmission methods. One of the benefits is high spectral efficiency (measured in bits/sec/Hz). The orthogonal OFDM mentions a precise mathematical connection between the frequencies of the sub channels that are applied in the OFDM technique. These frequencies are integer multiples of a basic frequency. This guarantees that a sub-channel does not intervene with other sub-channels despite the sub channels overlapping, which results in maximum spectral efficiency. OFDM has been implemented in IEEE 802.16a MAN/LAN and the IEEE 802.11a LAN standards. OFDM is also being considered in IEEE 802.20A, a standard in maintaining maximum BW connections for subscribers moving at speeds of up to 61 Mb/s. The IEEE 802.11a LAN standard works at raw data rates of up to 52 Mb/s (permit of channel conditions) with a 20-MHz channel spacing; therefore, the outcome will be 2.6 b/s/Hz BW efficiency. The real throughput is highly dependent on the MAC protocol. Moreover, depending on the conditions of the channel, IEEE 802.16a works in various ways through a data rate ranging from 4.21 to 22.91 Mb/s in a typical BW of 6.1 MHz.

1.3 MIMO

Multiple antennas can be used at the transmitter and receiver, an arrangement called a MIMO system. A MIMO system takes benefit of the spatial diversity in a dense multipath scattering environment that is obtained by spatially separated antennas. MIMO systems can be applied in a number of various ways to obtain either a diversity gain to combat signal fading or to obtain a capacity gain. In general, there are three types of MIMO techniques. The first type to increase the power efficiency by increasing spatial diversity. These approaches involve delay of diversity, STBC

[5,6] and STTC [7]. A layered approach is used by the second type to increase capacity. One popular example of such a system is V-BLAST proposed by Foschini et al [8]. where full spatial diversity is usually not achieved. Finally, the third type exploits the knowledge of channel at the transmitter. It decomposes the channel coefficient matrix using singular value decomposition and uses these decomposed unitary matrices as pre- and post-filters at the transmitter and the receiver to achieve near capacity [9].

1.4 MIMO-OFDM

Spatially multiplexed MIMO is known to increase the throughput, otherwise, The multipath character of the environment causes the MIMO channel to be frequency selective when much higher throughputs are aimed. OFDM can transform such a frequency-selective MIMO channel into a set of parallel frequency-flat MIMO channels and also increase the frequency efficiency. frequency-flat MIMO channels and also increase the frequency efficiency. Therefore, MIMO-OFDM technology has been researched as the infrastructure for next generation wireless networks [10]. Therefore, MIMO-OFDM, produced by employing multiple transmit and receive antennas in an OFDM system has become a practical alternative to a single carrier and SISO transmission [11]. However, Channel estimation becomes computationally more complex compared to SISO schemes due to an increase in the number of channels to be estimated. Using OFDM, information symbols are transmitted over many parallel independent sub-carriers using computationally efficient IFFT/FFT modulation/demodulation vectors. These MIMO schemes, combined with OFDM, have allowed for the easy transmission of symbols in space, time and frequency [12]. Various coding schemes have been developed to extract diversity from the channel. The seminal example is the STBC that could be used to extract spatial and temporal diversity [5].

1.5 Previous Work

The aim of this section is to present the related research in the field of Multiple Input Multiple Output Orthogonal and Frequency Division Multiplexing (MIMO-OFDM) systems using Orthogonal Space Time Block Coding (OSTBC):

- In 2018, Deshmukh, S. Bhosle, U. [13] analyzed and simulated MIMO-OFDM with various digital modulation systems such as BPSK, QPSK, and QAM implemented using Alamouti space-time block codes (STBC). STBC uses timeand spatial aspects to control error, unlike traditional ways which use the time dimension only. MIMO-OFDM using STBC with BPSK modulation was further simulated and analyzed for different antenna configurations. It was observed that as the number of antennas at the transmitter and receiver side rises, the diversity of the system increases and enhances bit error rate performance.

- In 2017, A. Agarwal and Saurabh N. Mehta [14] presented an overview of wireless MIMO-OFDM technology, which covered the advances in physical layer design, different time-space codes, frequency-space codes and interleaving to yield reduced bit error rate performance (BER) along with concatenated forward error correction methods.

- In 2016, Sudhir Sawarkar and Swati Dutta [15] compared the bit error rate efficiency of the 16-QAM and 64-QAM modulation methods with and without interleaving processes. Furthermore, the performance of the MIMO-OFDM system using the OSTBC coding technique was analyzed and compared with convolution coding.

- In 2014, A. Pandey and S. Sharma [16] compared OFDM technology performance using various modulation systems under the impact of AWGN and Rayleigh fading channel effects. In order to understand the impact of channel fading and to enhance efficacy of the BER value, OFDM signal simulations were performed with Rayleigh faded signals.

- In 2013, K. Chaudhar, D. Vishwakarma and A. Patel. [17] aimed to evaluate the efficiency of the BER parameter of MIMO-OFDM technology and MIMO for the AWGN channel along with a simulation channel with the support of BPSK and M-QAM modulation schemes.

1.6 Objectives

In this thesis, a simulation model is developed based on the fundamental architecture of the MIMO OFDM system. The performance of the MIMO OFDM system for various input modulation schemes (such as QPSK, 16 QAM and 64 QAM) under a

fading channel is analyzed using this model. Channel coding, such as convolutional coding, is one of the important elements determining the performance of the scheme. The initial attempt performed an analysis using the Rayleigh fading MIMO channel for the scheme with different input modulation types.

- Then, the system under the Rician fading channel is tested. Here, the entire process is repeated for different modulation techniques.
- The analysis of the MIMO-OFDM system using OSTBC (1 × 1, 2 × 2, 3 × 3 and 4 × 4) code structure is conducted, in which the first numeral refers to the number of transmitting antennas, and the second numeral refers to the number of receiving antennas. BER analysis is also included.
- For the fundamental model of OFDM systems, by adding the blocks of MIMO and OSTBC, simulation runs are performed for the most ideal channel, i.e., AWGN with the Rayleigh fading channel, at different modulation techniques and for different antenna configurations using OSTBC code structure, which are repeated.
- Similar to the study above, the system performance under the Rician fading channel is tested. The entire process is repeated for different antenna configurations and with different modulation techniques.

1.7 Organization of the Dissertation

This thesis consists of five chapters in total, structured as follows:

Chapter 1: Introduction, which consists of an introduction to the OFDM technique and its application, followed by a brief introduction to the MIMO system.

Chapter 2: This chapter presents how OFDM systems consist of the basic principles of the OFDM system, along with its advantages and disadvantages.

Chapter 3: In this chapter, we present how MIMO systems consist of a basic MIMO System model, MIMO with OSTBC and signal detection.

Chapter 4: This chapter presents the MIMO-OFDM system and consists of a detailed discussion of the study of MIMO-OFDM systems along with a number of modulation techniques and Space Time Coding techniques. In addition, the detection techniques for the MIMO-OFDM system is briefly discussed.

Chapter 5: Results and Discussions are presented with a discussion of the results simulated using MATLAB 2018a, starting with the Rayleigh channel and the Rician

channel for our model, for different modulation techniques and different antenna configurations. A complete analysis of BER is presented.

Chapter 6: In the final chapter, the conclusion of the thesis is presented, including a discussion of the results.

CHAPTER 2

OFDM SYSTEMS

2.1 Introduction

Orthogonal Frequency Division Multiplexing (OFDM) is a multicarrier multiplexing method that divides a wideband into many narrow bands. OFDM is one of the most common techniques for a parallel-data-transmission scheme, which reduces the effect of multipath fading and makes complex equalizers redundant. Based on the principle of modulating each data stream on subcarriers, OFDM divides high-bit data streams in to several lower bit rate data streams. The input data are separated into parallel streams, every narrow-band modulating a different subcarrier. The narrow-band waveforms have sidebands that overlap, but they are orthogonal to each other. Because the wideband is de-multiplexed into several narrow-bands, it allows the scheme to increase the throughput of a system by multiplexing large amounts of data. One OFDM symbol block comes from a sum of these narrowband waveforms. To guard the symbol blocks from interfering with one another through a channel, a cyclic prefix (CP) is used, which must be of the order of the channel delay spread. The proportion of time occupied by the CP represents an overhead. However, the effective data rate of an OFDM technique is high with very good spectral efficiency. OFDM is widely used in the design of wireless communication techniques, such as wireless fidelity (Wi-Fi) [18], worldwide Interoperability for microwave access (WiMAX) [19-21], satellites [22], Long-Term Evolution (LTE) [23], LTE-Advanced [24,25], digital audio and video broadcasting (DAB/DVB) [26], etc. OFDM is traditionally designed using the Fast Fourier transform (FFT), a computationally efficient tool that implements the Discrete Fourier Transform (DFT) [27]. Variations of OFDM using the wavelet transform (WT) also have applications in power line communications (PLCs) [28].

2.2 Brief History of OFDM

Bell laboratories, in the late 1960s, studied channel partitioning to generate a finite set of parallel independent sub-channels [29]. In 1966, Chang of Bell laboratories exploited this to propose the first OFDM scheme for dispersive fading multi-channel data transmission and received a patent in 1970 [30, 31]. In 1971, Ebert and Weinstein introduced the DFT to replace the bank of sinusoidal generators required in the modulators and demodulators of the equivalent frequency division multiplexing (FDM) systems [32]. The DFT realized the FDM to create orthogonal waveforms using the FFT [32]. The DFT generates time domain orthogonal waveforms using the inverse-FFT (IFFT) in the transmitter and FFT in the receiver. These were used with a guard interval [32]. In 1985, OFDM was suggested to be used in mobile communications [21] and it was adopted in digital subscriber lines (DSLs) in 1993 [19]. In 1997, OFDM was proposed for DVB-terrestrial (DVB-T) by the European Telecommunications Standard Institute (ETSI) and in Wi-Fi wireless local area networks (WLANs) (e.g., IEEE 802.11g) in 1999 [21]. Currently, OFDM is used in DAB, wireless personal networks (PANs) such as IEEE 802.15.3a and other Wi-Fi WLANs such as IEEE 802.11a/n [18-26]. In long distance wireless transmissions to support mobile Internet services such as WiMAX (e.g., IEEE 802.16d-2004 and IEEE 802.16e-2005, both amended in 2006 as IEEE 802.16m), OFDM is used [33-34]. In fact, WiMAX was the first cellular standard to employ OFDM [35]. WiMAX supports mobility up to 120 km/hr. and uses space-time block coding [35]. OFDM renovated the FDM used in 1G generation cellular systems, and it has been proposed for LTE and LTE-Advanced. Compared to FDM, OFDM saves 50% of the transmission bandwidth [31].

2.3 Basic Principle of OFDM Signalling

OFDM is a special type of multi-carrier modulation (MCM) which enables multiple access with overlapping spectra and densely spaced sub-carriers. MCM operates on the concept of transmitting data by splitting streams into separate bit streams. These sub-streams are used to modulate several carriers with much lower BER. This method is being implemented as the next generation transmitting technique for mobile wireless networks. Bandwidth is divided in several non-overlapping sub-carriers during multicarrier transmissions. The signal of the sub-carriers is

orthogonal if the inner product of any two of the sub-carriers is zero, as shown in Figure 1.

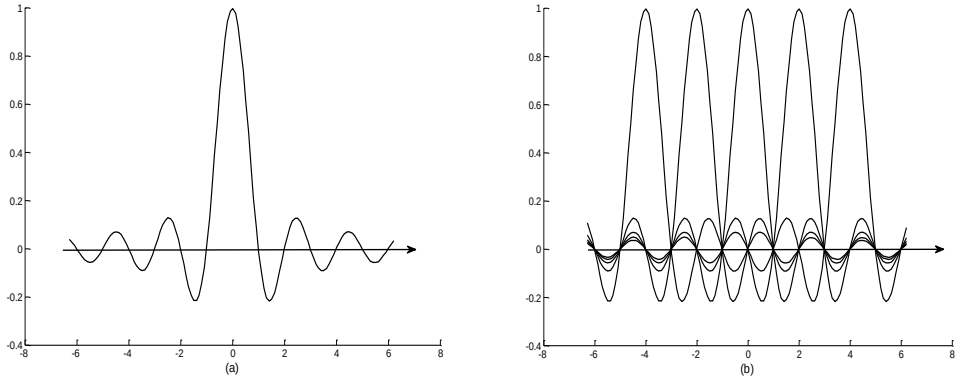

Figure 1: Spectra of (a) an OFDM sub-channel, and (b) an OFDM signal .

The sub-channels overlap each other to a certain extent in OFDM. This can be seen in Figure 1(b), that contributes to the effective use of the total bandwidth. The data sequence is mapped into symbols, one symbol per channel, that are distributed and sent over the N sub-channels. The carrier frequencies must be carefully selected to allow dense packing and still ensure that there is the lowest interference between the sub-channels. Using orthogonal carriers, which can be viewed in the frequency domain, the distance to the first spectral null is given as the frequency distance between the two sub-carriers. Although the OFDM concept was developed in the 1960s, it was not feasible until the advent of FFT. It became possible to generate OFDM using the digital domain for sub carrier orthogonality with the advent of FFT/IFFT. The data symbol of N complex-valued modulates N orthogonal carriers using the IFFT forming .

The transmitted OFDM signal multiplexes N low-rate data streams, every experiencing an almost flat fading channel when transmitted. In single carrier systems every symbol occupying an entire bandwidth could be lost due to frequency selective fading, but when transmitted on low data parallel streams, channel become flat fading and symbol time increases [20]. The block diagram of OFDM scheme is shown Figure 2.

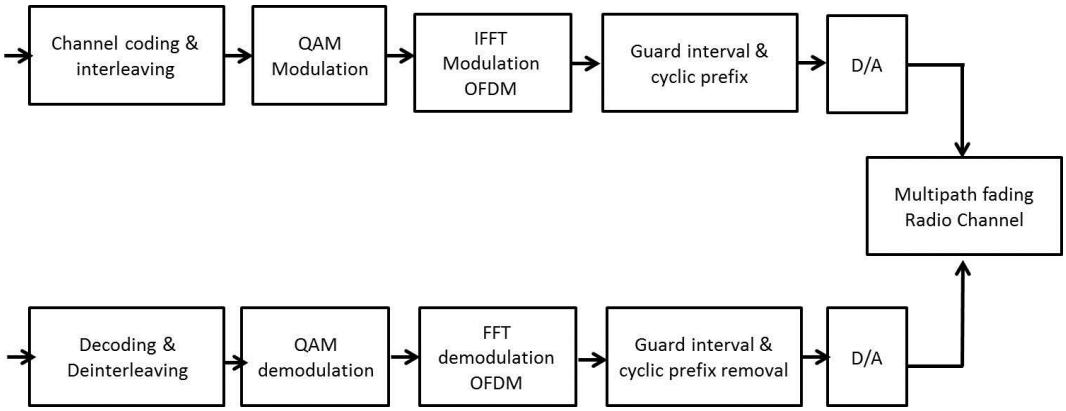

Figure 2: Block Diagram of OFDM using FFT and IFFT.

Essentially, OFDM technology is based on three facts:

- ⇨ The IFFT and FFT are applied to modulate and demodulate separate OFDM sub-carriers to change the signal spectrum to the time domain for transmission across the channel and to recover data symbols in serial order using FFT at the receiving end.
- ⇨ The cyclic prefix (CP) is used as a Guard Interval. CP keeps the signal being transmitted periodically. The avoidance of intercarrier interference (ICI) is one of the reasons for applying CP.
- ⇨ Interleaving is the most significant concept used. The radio channel may influence the data symbols transmitted on one or more sub carriers which lead to bit errors . To encounter this problem we use effective coding techniques [37].

2.3.1 Serial to Parallel Conversion

Data transmission normally happens in the serial stream of bits. Data transmitted in parallel streams in OFDM, so that a serial to the parallel stage is needed to convert the input bit stream to data transmitted on OFDM symbols. The data to be sent on every OFDM symbol depends on the modulation scheme used and on the number of carriers used [38].

2.3.2 Modulation

In OFDM, Quadrature Phase-Shift Keying Modulation (QPSK) is applied to transfer the information through different sub-channels. In order to obtain high spectral efficiency, QAM or other higher-order modulation techniques can be applied. The

selection of modulation depends on transmission quality and data rate requirements [39].

2.3.3 Fast Fourier Transform (FFT)

The initial complexity of the OFDM system is reduced by the Fourier Transform application, where Fourier and Inverse Fourier transforms are used in harmonic-related frequencies for OFDM systems. However, the common method of the Fourier transform is a Discrete Fourier Transform (DFT) which operates in all digital techniques with discrete values. FFT is an effective and quick way to calculate the DFT applied in OFDM. In OFDM, the serial data is reshaped in the parallel form. The data is grouped in specific size as per OFDM design and will be converted to complex numbers. A complex number is then modulated using IFFT. On the receiving end the data is again reshaped from parallel to serial for transmission [39,40].

2.3.4 Guard Interval (GI)

Due to multipath propagation, GI is introduced in OFDM as it affects the symbols to delay and attenuate, which causes ISI. In GI, a CP is applied within an OFDM frame to counter ICI. The CP is basically a copy of the last symbols of the OFDM signal placed first, generating a periodic signal in the receiver, as shown in Figure 3.

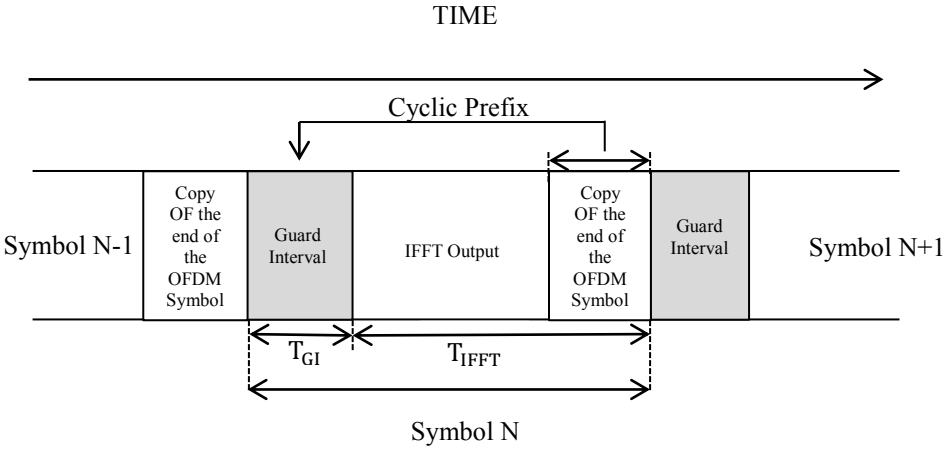

Figure 3: Guard Interval and Cyclic Prefix.

where: T_{GI} is Guard Interval time period and T_{IFFT} is IFFT time period for the OFDM signal. Before demodulating the OFDM signal the CP must be removed. By

exploiting the structure imposed using CP. Symbol synchronization can be achieved. The IDFT and DFT can be used for modulation and demodulation of the signal due to the orthogonality of the carrier [14].

2.3.5 Interleaving

Interleaving is one of the best methods to enhance the BER. In OFDM, transmitted data are separated into many sub-carriers. Therefore, every sub-carrier will connect flat fading and here the GI is used. Channel frequency response induces data loss and a deep fade when propagating over the channel in a burst. In order to solve this problem, a good method is required to recover data and handle burst errors. Data are reclassified from burst errors to random errors in an interleaving process and can be easily recovered from the receiver. Bits are reconfigured in a manner such that reverse reclassification is used to retrieve data at the original receiver, leading to a random error. One approach that is widely used for interleaving is block codes where data are written row by row and then recovered column by column [36].

2.3.6 Windowing

The FFT of the square wave is the sine function. A square pulse has a very large bandwidth due to its side lobes. The FFT of these side lobes will result in a sharp transition of bits, which causes spreading of the signal into the neighboring spectrum in addition to a leakage of energy. Windowing is the technique which causes the symbol or signals to decrease in order to reside in the spectrum. In OFDM, windowing is performed on every symbol and it must not affect the signal. Hence, the result is a pulse shaped wave [36].

2.3.7 Peak to Average Power Ratio (PAPR)

There are a number of sub-carrier frequencies in the OFDM signal that give a significant PAPR if added coherently. An amplitude of signals equal to N times the average power is obtained when signals are applied in the same phase. In a non-linear region or in saturation, signals with a large PAPR transmit over the amplifier to be processed and migrated. Thus, the system shows non-linear performance, which influences the efficiency of the output signal with the amplifier being deformed.

Three techniques are available to minimize PAPR:

⇨ Distortion of Signals

⇨ Techniques for Coding

⇨ Techniques of Scrambling

The reduction in PAPR leads to improvements in the signal-to-noise ratio at the receiver. This also needs the transmission of high average power [36].

2.4 Mathematical description

A collection of closely separated FDM subscribers can be used as an OFDM signal. In the frequency domain, each sub-carrier transmitted results in a spectrum of sinc feature with side lobes that generate overlapping spectra between sub-carriers. This will cause sub-carrier interference at orthogonally spaced frequencies. At orthogonal frequencies, the individual peaks carriers align with the nulls of every other sub-carrier. This overlap of spectral energy does not interfere with the system's ability to recover the original signal. The receiver multiplies the incoming signal by the known set of sinusoids to recover the original set of bits which are sent. The use of orthogonal sub-carriers simplifies a large number of sub-carriers per BW, which will result in a rise in spectral performance. Orthogonality avoids interference between overlapping carriers in a perfect ODFM signal, which is also defined as intercarrier interference. In OFDM schemes, if there is a loss of orthogonality, the sub-carriers intervene with each other.

If N sub-carriers are used and every sub-carrier is modulated using M-ary signaling, the ODFM symbol alphabet consists of one out of M^N number of combined symbols. The low-pass equivalent OFDM signal can be represented as:

$$x(t) = \sum_{k=0}^{N-1} X_k \, e^{j2\pi kt/T_s} \qquad 0 \le t < Ts \tag{2.1}$$

where:- X_k are the data symbols.

T_s is the OFDM symbol time.

N is the number of sub-carriers.

The sub-carrier spacing of $\frac{1}{T_S}$ makes the symbols orthogonal over every symbol period, this property can be expressed as:

$$\frac{1}{T_s}\int_0^{T_s} (e^{j2\pi k_1 t/T_s})^* (e^{j2\pi k_2 t/T_s})\, dt = \frac{1}{T_s}\int_0^{T_s} (e^{j2\pi (k_2-k_1) t/T_s})\, dt = \delta_{k_1 k_2} \tag{2.2}$$

where $(e^{j2\pi k_1 t/T_s})^*$ is the complex conjugate operator. A guard interval of length T_g is introduced prior to the OFDM block in order to stay away from ISI in multipath fading channels. A cyclic prefix of OFDM variants 20 is transmitted through this interval as the signal in the interval equals the signal in the interval $-T_g \leq t < T_s$. The OFDM signal with cyclic prefix can be presented as:

$$x(t) = \sum_{k=0}^{N-1} X_k \, e^{j2\pi kt/T_s} \qquad -T_g \leq t < T_s \qquad (2.3)$$

Equation 2.3 represents the low-pass signal. It can be either real-valued or complex-valued. Real-valued low pass equivalent signals are typically transmitted at baseband wire line applications such as DSL. For wireless applications, the low-pass signal is typically complex-valued. In this case, the transmitted signal is up-converted to a carrier frequency f_c. In general, the transmitted signal can be represented as:

$$s(t) = \mathrm{Re}\{x(t)e^{j2\pi f_c t}\} = \sum_{k=0}^{N-1} |X_k| \cos(2\pi[fc + k/Ts]t + \arg[X_k]) \qquad (2.4)$$

where s(t) is a time-domain signal being transmitted. Sub-carrier separation of $\frac{k}{T_s}$ verifies the orthogonality between the sub-carriers.

2.5 Advantages of OFDM

OFDM evolved with many advantages. These are listed as follows:

- ⇨ The effective technique of dealing with multipath fading channels is OFDM.
- ⇨ It has enhanced throughput.
- ⇨ In OFDM, systems equalization greatly decreases complexity and it becomes simpler at the receiver.
- ⇨ Low receiver complexity with simple implementation of FFT [30].
- ⇨ Due to orthogonality between the sub-carriers, the OFDM system provides high spectral efficiency.
- ⇨ OFDM is suitable for single-frequency broadcasting applications.

2.6 Disadvantages of OFDM

OFDM has evolved with many disadvantages, which are listed as follows:

- ⇨ Compared to single carrier modulation, there is a higher peak-to-average-power ratio (PAPR), which decreases the power efficiency of the RF amplifier.
- ⇨ OFDM is much more sensitive to phase noise and frequency offsets.
- ⇨ It has high ICI sensitivity [13].

- ⇨ Although CPs are used to overcome ISI, OFDM wastes available bandwidth in proportion to the CP length used.
- ⇨ Due to the CP, there is a reduction in effective transmit power since part of the signal power is used to drive the CP.
- ⇨ There is increased noise overhead proportional to the CP.
- ⇨ CP adds additional computational time to the system.

CHAPTER 3

MIMO SYSTEMS

3.1 Introduction

Multiple antennas at the transmitter side and at the receiver side through a channel are describe as a Multiple-Input-Multiple-Output (MIMO), while the Signal-Input-Signal-Output (SISO) channel has only one antenna at the transmitter side and only one antenna at the receiver side. In addition to increased reliability achieved by diversity, higher data rates produced through spatial multiplexing are the significant benefits of the MIMO scheme [42]. These two concepts are used in MIMO schemes together. The same information is transmitted over multiple transmission antennas during a diversity system and received at multiple receive antennas at the same time. During a diversity technique, equal data is transmitted over multiple transmit antennas and received by many antennas simultaneously. Because the fading is taken into account for each link between a pair of transmit and receive antennas to be independent, the same information is transmitted through various paths. If one path is not clear , a copy of data received through the other path could be good. Therefore, The probability of correctly detecting the data increases. The block diagram of MIMO System is shown Figure 4.

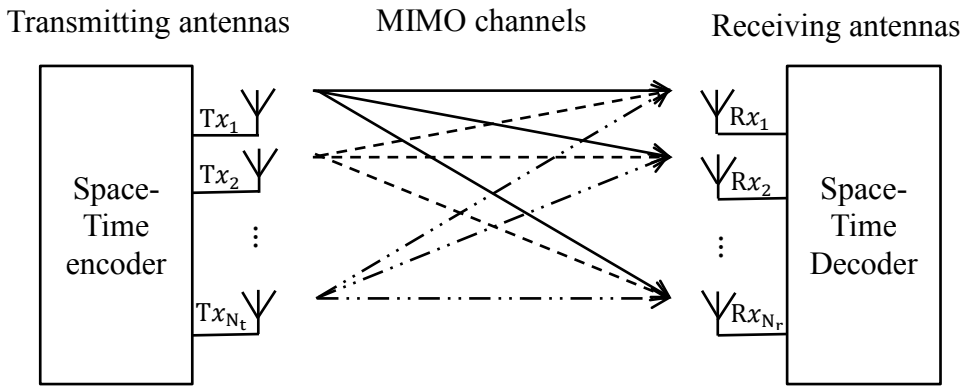

Figure 4: Block Diagram of MIMO System

MIMO technology is a wireless technology that uses different transmitters and receivers to transmit more data simultaneously. MIMO technology takes benefit of a multipath radio wave case where transmitted data falls back on the walls and on the other side, reaching the receiving antenna several times at various angles and at slightly various times. The MIMO wireless system is able to significantly increase the capacity of a given channel as a result of the use of multiple antennas. By increasing the number of transmit and receive antennas it is possible to linearly increase the throughput of the channel with each pair of antennas added to the system. This makes the wireless MIMO scheme one of the most important wireless systems to be used in in the next generations of communications. As spectral bandwidth becomes an increasingly important asset for radio communication systems, systems are required to allow more effective use of the available bandwidth.

3.1.1 Single Input Single Output (SISO)

The simplest form of radio link can be determined in MIMO terms as SISO – Single Input Single Output – as shown in Figure 5. This transmitter works with only one antenna at the receiver side. There is no extra processing and no diversity is needed.

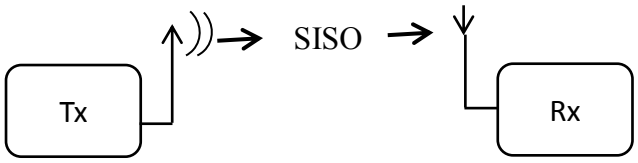

Figure 5: SISO - Single Input Single Output

Simplicity is a benefit of the SISO technique. SISO does not need to be processed in terms of the various types of diversity that can be implemented. The performance of the SISO channel is limited as fading and interference will affect the method more than the MIMO technique using the various types of diversity. Throughput depends on the SNR and channel bandwidth.

3.1.2 Single Input Multiple Output (SIMO)

SIMO, or Single Input Multiple Output, version of MIMO occurs where the transmitter has only a single antenna and the receiver has multiple antennas. This

creates diversity at the receiver. It is frequently used to support receiver systems receiving signals from a number of independent sources to decrease the effects of fading. SIMO has been used for many types of communication systems through short wave receiving stations to decreasing the impacts of interference and ionospheric fading. The block diagram of SIMO System is shown Figure 6.

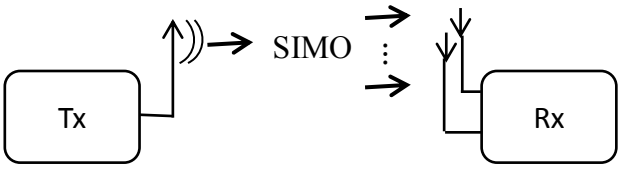

Figure 6: SIMO - Single Input Multiple Output

The benefit of SIMO is relatively simple in its application although it has a number of drawbacks in that the processing is needed at the receiver. The use of SIMO may be completely suitable in several communication systems. However, where the receiver is set in a mobile device, such as a mobile phone, the level of processing can be restricted by battery drainage, cost and size. Two methods of SIMO that can be used may be:

- ⇨ Maximum ratio combining: This form of SIMO takes every signal and sums them to give them a combination. In this way, the signals from every antenna contribute to the overall signal.
- ⇨ Switched diversity: This method of SIMO explores the strongest signal and switches to that antenna.

3.1.3 Multiple Input Single Output (MISO)

Multiple-Input-Single-Output (MISO) is also called transmit diversity as shown in Figure 7. The same data are transmitted from two or more transmitter antennas and the receiver is then able to receive the optimum signal which is used to receive and extract the required data.

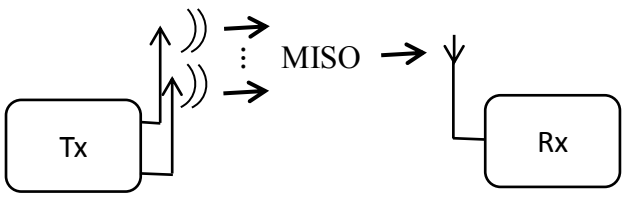

Figure 7: MISO - Multiple Input Single Output

The benefit of using MISO is that the multiple antennas and increased processing are moved from the receiver to the transmitter. In cases such as cellphone UEs, this can be a significant improvement in terms of space for the antennas and it decreases the level of processing required in the receiver for the redundancy coding. This has a positive effect on cost, battery life and size as the lower level of processing requires lower battery consumption.

3.1.4 Multiple Input Multiple Output (MIMO)

MIMO is essentially a radio antenna system that includes multiple transmitter and receiver antennas to allow a variety of signal paths to carry data, selecting various paths for each antenna to allow multiple signal paths to be used.

Figure 8: MIMO - Multiple Input Multiple Output

The basic block structure of the MIMO system is shown in Figure 8. One of the most important principles behind MIMO wireless systems space-time signal processing during which time is complemented with the spatial dimension inherent within the use of multiple spatially distributed antennas. The use of multiple antennas positioned at various points, for example. Accordingly MIMO wireless systems are often viewed as a logical extension to the smart antennas that have been used for several years to improve wireless communication systems. The signal can take several paths between a transmitter and a receiver. In addition, the paths used will change even a small distance by moving the antennas. the variability of paths available occurs as a outcomes of the amount of objects that appear to the side or maybe within the direct path between the transmitter and receiver. These multiple paths previously served only to introduce interference. By using MIMO, these additional paths are often wont to benefit. they will be used to provide additional robustness to the radio link by improving the SNR or by increasing the link data capacity.

3.2 Benefits of MIMO technology

3.2.1 Array gain

Array gain is the average rise in the SNR at the receiver side emerging from the coherent combining impact of multiple antennas at both sides of the receiver and transmitter or at either the transmitter or receiver side. The transmitter places the transmission weights, depending on the channel factors if the channel is known in the multiple antenna transmitters in order to ensure that the single antenna receiver has a coherent combination. In such a case, the array gain is called transmitter array gain.

Alternatively, if we have only one antenna at the transmitter and a multiple antenna receiver and no information about the channel that has perfect information about the channel, then the receiver can aptly weight the arriving signals so that they will be combined coherently at the output. As a result, the signal will improve. This is the SIMO case and is called receiver array gain. For the most part, several antenna systems need perfect knowledge for a channel either at the transmitter or the receiver or both to obtain this array gain.

3.2.2 Interference reduction and avoidance

Interference in wireless communication networks outcomes from multiple users sharing time and frequency resources. Interference may be mitigated in MIMO schemes by exploiting the spatial dimension to increase the separation between users. For example, in the presence of interference, array gain increases the tolerance to noise as well as the interference power, hence improving the signal-to-noise-plus-interference ratio (SINR). Additionally ,the spatial dimension may be leveraged for the purposes of interference avoidance, i.e., directing signal energy towards the intended user and minimizing interference to other users. Interference reduction and avoidance increase the coverage and range of a wireless communication network.

3.2.3 Diversity gain

Multipath fading is a significant problem in wireless communications. In a fading channel, signal experiences fades (i.e they fluctuate in their strength). When signal power drops significantly, the channel is said to be in deep fade. Here, diversity is used to combat fading. This includes providing copies of the transmitted signal through frequency, space or time.

3.3 MIMO Techniques and channel models

MIMO techniques can be categorized into three main types, the first of which uses spatial multiplexing to achieve capacity gain. The second type uses coding techniques to provide spatial diversity, such as space-time block codes. The third type exploits the knowledge of the channel and de-correlates the channel matrix so as to minimize interference among antennas, namely, precoding. In the following section, the encoding strategies at the transmitter for these three types of techniques are presented. They can be applied directly to each sub-carrier in the MIMO schemes.

To introduce MIMO channel models, we begin with the process of signal transmission from a transmitter to a receiver (SISO case). A signal transmitted through wireless media from a transmitter undergoes physical processes such as refraction, reflection, diffraction and scattering on its way to the receiver in the channel [43]. In the process, the received signal is a group of multiple copies of the same signal received through multiple paths after experiencing multiple physical processes. Most of the time, the delays of all the received multipath components are negligible compared to the bit/symbol duration. All the multipath components have undergone some physical process. Therefore, they arrive at the receiver with different magnitudes and different phases. In general, all the received multipath components can be decomposed into in-phase (real) and quadrature phase (imaginary) components. Thus, the received signal is a sum of the in-phase components and quadrature phase components of the received multipath copies. All these components have random magnitudes and phases. Therefore, real and imaginary components can be assumed to be random variables with either a positive sign or a negative sign. In practice, when the number of multipath components is sufficiently large with no dominant component, both the resultant components (real and imaginary) can be assumed to follow a Gaussian distribution by applying the Central Limit Theorem [44]. The envelopes of such channels are known to be Rayleigh distributed. In such a case, the received signal is given as:

$$\mathrm{r} = \mathrm{Hx} + \mathrm{n} = \begin{bmatrix} \mathrm{r}_1 \\ \mathrm{r}_2 \\ \vdots \\ \mathrm{r}_{\mathrm{N_r}} \end{bmatrix} = \begin{bmatrix} \mathrm{h}_{11} & \mathrm{h}_{12} & \cdots & \mathrm{h}_{1\mathrm{N}_1} \\ \mathrm{h}_{21} & \mathrm{h}_{22} & \cdots & \mathrm{h}_{1\mathrm{N}_2} \\ \vdots & \vdots & \ddots & \vdots \\ \mathrm{h}_{\mathrm{N}_{r1}} & \mathrm{h}_{\mathrm{N}_{r2}} & \cdots & \mathrm{h}_{\mathrm{N_rN_t}} \end{bmatrix} \begin{bmatrix} \mathrm{x}_1 \\ \mathrm{x}_2 \\ \vdots \\ \mathrm{x}_{\mathrm{N_t}} \end{bmatrix} + \begin{bmatrix} \mathrm{n}_1 \\ \mathrm{n}_2 \\ \vdots \\ \mathrm{n}_{\mathrm{N_r}} \end{bmatrix} \tag{3.1}$$

where H is the channel coefficient.

x is the transmitted bit/symbol.

n is the additive noise.

r_i is the signal received at the i^{th} receiving antenna.

x_i is the symbol transmitted through the i^{th} transmitting antenna.

h_{ij} is the complex channel coefficient between j^{th} transmit antenna and i^{th} receive antenna.

Considering the MIMO system model shown in Figure 8, we can see that it contains N_t antennas at the transmitter and N_r antennas at the receiver. Throughout the text, we refer to such MIMO systems as $N_t \times N_r$ MIMO systems, for which there will be a total of $N_t \times N_r$ links from the transmitter to the receiver. Hence, the channel coefficient would no longer be a single element as in the SISO case. Now, the channel can be represented as a matrix of dimension $N_t \times N_r$ and the received signal would be a vector of dimension $N_r \times 1$, which given as Equation 3.1 where H is the channel matrix containing $N_t \times N_r$ complex elements, x the transmitted vector of dimension $N_t \times 1$ and n the additive noise vector of dimension $N_r \times 1$, thus:

Channel modeling is an essential requirement to analyze various performance metrics of wireless communication systems. In most cases, it is assumed that the received signal is a collection of many multipath components generated as a result of reflections, diffraction or scattering from various obstacles in the path between the transmitter and receiver. As a result, the real and imaginary part of the channel can be modeled as Gaussian distributed. The magnitude of gain of such channels follows the distribution of Rayleigh. These channels are also known as Rayleigh fading channels.

MIMO systems can be classified as open loop MIMO systems or closed loop MIMO systems based on the scheme that is used for the transmission of information. Some transmission schemes need a feedback link from the receiver to the transmitter to provide information about channel states or some parameter of channel matrix. Such MIMO systems requiring feedback links are known as closed loop MIMO systems, while those MIMO systems, which do not require any information at the transmitter, back from the receiver, are known as open loop MIMO systems.

3.3.1 Spatial multiplexing

Spatial multiplexing provides a linear in min (N_r, N_t) increase within the capacity or the number of transmit and receive antenna pairs for an equivalent BW and with no extra power expenditure. This is only possible in MIMO channels. Consider the cases of two receive and two transmit antennas which are expanded to more common MIMO channels.

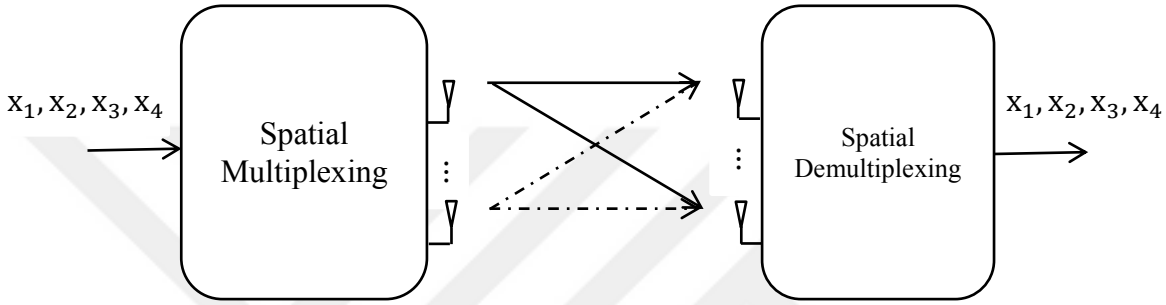

Figure 9: Spatial Multiplexing

The basic block structure of the MIMO spatial multiplexing system is shown in Figure 9. The bit stream is split into two half-rate bit streams, modulated and transmitted at the same time from both the transmitter and receiver antennas. The receiver, having complete knowledge of the channel, recovers these separate bit streams and combines them to recover the first bit stream. As the receiver has knowledge of the channel, it provides receiving diversity, but the method has no transmitted diversity since the bit streams are completely different from one another and carry completely different data. Thus, spatial multiplexing increases the transmission rates correspondingly with the number of transmit and receive antenna pairs.

3.3.2 Space time block codes

Spatial multiplexing is known for improving the capacity and spectral efficiency in the rich scattering environment. However, it does not provide any diversity gain at the transmitter. The diversity gain of spatial multiplexing systems depends only on the number of antennas available at the receiver. In 1998, Alamouti proposed a transmission scheme for MIMO systems to obtain transmit diversity at the same time

as a simple decoding scheme for MIMO wireless systems [45]. However, the scheme explores the spatial and temporal aspects of diversity schemes and it achieves full diversity order. The scheme is known as Space-Time Block Coding (STBC).

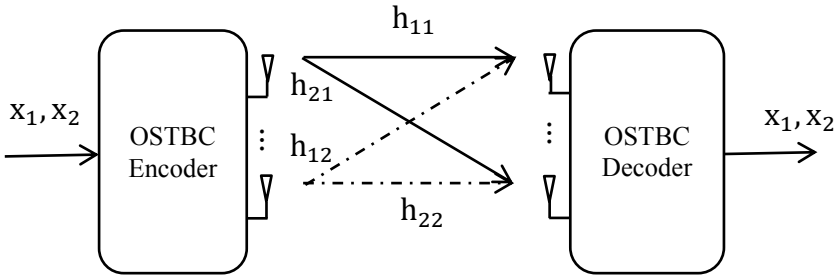

Figure 10: OSTBC System

A block diagram of an OSTBC system is shown in Figure 10. As the name suggests, an appropriate coding scheme is used at the transmitter to encode the information before it is transmitted. The coding scheme uses a block of incoming data bits and transmits it across the transmitting antennas which are separated in space. Hence, it is named space-time block code (STBC). In STBC systems, information is transmitted in blocks. An STBC symbol can be mathematically expressed as:

$$S = \begin{bmatrix} s_{1,1} & \cdots & s_{1,n} \\ \vdots & \ddots & \vdots \\ s_{r,1} & \cdots & s_{r,n} \end{bmatrix} \tag{3.2}$$

where r is the blocks of symbols, n is the time slots for one block and s_{ij} is one of the symbols.

The transformation here may be a negation, a complex conjugate or a negation of a complex conjugate in accordance with the designed code.

The maximum code rate which can be achieved in STBC systems is 1; i.e., it does not achieve a gain in spectral efficiency. An STBC system that can achieve the maximum code rate is known as a full rate STBC system. However, this scheme is more interesting as far as diversity order and receiver complexity are taken into consideration. To understand the STBC transmission scheme, we start with the Alamouti STBC scheme for 2×1 MISO systems. In this case, the channel matrix becomes a row vector thus:

$$H = [h_{11}\ h_{12}] \tag{3.3}$$

Two transmit antennas are available. They transmit digitally modulated symbols at the same time. Two symbols are transmitted in two time slots that makes the Alamouti scheme a full rate STBC system. Let two consecutive digitally modulated symbols from the incoming data bits at any time be s_1 and s_2. These symbols are transmitted as:

$$x_1 = \begin{bmatrix} s_1 \\ s_2 \end{bmatrix} \text{ and } x_2 = \begin{bmatrix} -s_2^* \\ s_1^* \end{bmatrix} \quad (3.4)$$

in first and second time slots respectively. Therefore, in general, when s_1 and s_2 are the digitally modulated symbols to be transmitted, the STBC symbol transmitted may be given as:

$$X = [x_1 \quad x_2] = \begin{bmatrix} s_1 & -s_2^* \\ s_2 & s_1^* \end{bmatrix} \quad (3.5)$$

The signal received in separate time slots of the transmission, r_1 and r_2, are represented as:

$$r_1 = h_{11}s_1 + h_{12}s_2 + n_1 \quad (3.6)$$

$$r_2 = -h_{11}s_2^* + h_{12}s_1^* + n_2 \quad (3.7)$$

To recover the transmitted symbols, it is assumed that the channel state information is available at the receiver. For detection of s_1 and s_2, the following computations are performed.

$$\hat{s}_1 = h_{11}^* r_1 + h_{12} r_2^* \quad (3.8)$$

$$\hat{s}_2 = -h_{11} r_2^* + h_{12}^* r_1 \quad (3.9)$$

The substitutions of the above operation results in the following relations:

$$\hat{s}_1 = (\|h_{11}\|^2 + \|h_{12}\|^2)s_1 + h_{11}^* n_1 + h_{12} n_2^* \quad (3.10)$$

$$\hat{s}_2 = (\|h_{11}\|^2 + \|h_{12}\|^2)s_2 + h_{11} n_2^* + h_{12}^* n_1 \quad (3.11)$$

We consider the Alamouti STBC scheme for 2 × 2 MIMO scheme. In this case, the channel matrix becomes:

$$H = \begin{bmatrix} h_{11} & h_{12} \\ h_{21} & h_{22} \end{bmatrix} \quad (3.12)$$

The first row corresponds to the links from the transmitter antennas to the first receiving antenna and the second row corresponds to the links from transmitter antennas to the second receiving antenna. The signals received by the first antenna in separate time slots of the transmission, r_{11} and r_{12}, are given as:

$$r_{11} = h_{11}s_1 + h_{12}s_2 + n_{11} \quad (3.13)$$

$$r_{12} = -h_{11}s_2^* + h_{12}s_1^* + n_{12} \quad (3.14)$$

And the signals received by the second antenna in the respective time slots of the transmission r_{21} and r_{22} are given as:

$$r_{21} = h_{21}s_1 + h_{22}s_2 + n_{21} \quad (3.15)$$

$$r_{22} = -h_{21}s_2^* + h_{22}s_1^* + n_{22} \quad (3.16)$$

For the detection of s_1 and s_2, after implementing the technique discussed for the single receiver antenna individually on the signals received on the first and second receiver antenna, we have:

$$\hat{s}_{11} = (\|h_{11}\|^2 + \|h_{12}\|^2)s_1 + h_{11}^* n_{11} + h_{12}n_{12}^* \quad (3.17)$$

$$\hat{s}_{12} = (\|h_{11}\|^2 + \|h_{12}\|^2)s_2 - h_{11}n_{12}^* + h_{12}^* n_{11} \quad (3.18)$$

$$\hat{s}_{21} = (\|h_{21}\|^2 + \|h_{22}\|^2)s_1 + h_{21}^* n_{21} + h_{22}n_{22}^* \quad (3.19)$$

$$\hat{s}_{22} = (\|h_{21}\|^2 + \|h_{22}\|^2)s_2 - h_{21}n_{22}^* + h_{22}^* n_{21} \quad (3.20)$$

From the above expressions, s_1 and s_2 can be detected as follows.

$$\hat{s}_1 = (\|h_{11}\|^2 + \|h_{12}\|^2 + \|h_{21}\|^2 + \|h_{22}\|^2)s_1 + h_{11}^* n_{11} + h_{12}n_{12}^* + h_{21}^* n_{21} + h_{22}n_{22}^* \quad (3.21)$$

$$\hat{s}_2 = (\|h_{11}\|^2 + \|h_{12}\|^2 + \|h_{21}\|^2 + \|h_{22}\|^2)s_2 - h_{11}n_{12}^* - h_{12}^* n_{11} - h_{21}n_{22}^* + h_{22}^* n_{21} \quad (3.22)$$

Again, from the above expressions, it can be observed that the symbols s_1 and s_2 are separated, and both the expressions contain $\|h_{11}\|^2 + \|h_{12}\|^2 + \|h_{21}\|^2 + \|h_{22}\|^2$. This means that among the four channels, when any single link is strong, it reduces the probability of error in the detection at the receiver. Thus, it is observed that the system offers full diversity order of $N_t \times N_r$, which is 4 in the present system under consideration. In the examples presented here, we have considered two transmit antennas, which is the requirement for the Alamouti STBC. However, many other space-time codes use a different number of antennas at the transmitter.

CHAPTER 4

MIMO-OFDM SYSTEMS WITH FECs

4.1 Introduction

In the previous chapter, the principal theory of the MIMO system and OFDM modulation were discussed. In this chapter, the combination of MIMO communication wireless systems and OFDM systems is analyzed. This approach is considered to be the most popular [46]. The combined MIMO-OFDM method has benefits including the improved spectral efficiency of OFDM [47], the high reliability of links that create more antennas and greater BW support, which leads to high performance as well as higher data rates and it has larger utilization in high-speed wireless transmission [48]. The increase in the transmission bandwidth efficiency of the combined MIMO-OFDM has been studied during estimating the blind channel of the system [49]. For reliable transmission of signals in the MIMO scheme, STBC has been developed. Generally, the error-correcting codes produce a threshold effect that gradually reduces the performance at the low SNR range [50]. In the transmitting antennas, orthogonal space-time block codes (OSTBC) are used [51]. It exhibits the property of diversity, but there is no coding gain. Hence, OSTBC that is concatenated with MIMO-OFDM has been used to provide diversity in both space and time [52, 53]. The concatenation scheme includes an inner OSTBC code and an outer channel code. The BER performance of the MIMO-OFDM using OSTBC has been evaluated by not concatenating with the channel codes [54−55]. The Convolution code is a technique of channel coding that is concatenated with Alamouti STBC under different fading conditions [54]. The efficiency of the Convolution Code with MIMO OFDM systems has been analyzed without channel correlation [56]. The MIMO-OFDM scheme with a description of FECs, which have been applied to wireless communications and have been used as a way to control and correct errors

generated during video distribution. FEC codes involve the Convolution Code, Reed-Solomon and Interleaving. The concatenated error correction code method, termed as Convolution Code, Reed-Solomon and Interleaving with the Alamouti code MIMO-OFDM, was studied through different fading conditions, such as the Rayleigh and Rician fading channels.

4.2 Randomization

The random distribution of data is achieved on every burst of data on the downlink and uplink, which means that the random distribution must be used separately for every allocation of a data block. The preambles are not randomized. If the quantity of data being transmitted does not fit closely to the quantity of data allocated, only a "1" padding will be added to the end of the transmission block. For each new allocation, the shift-register of the randomizer will be initialized. The pseudo-random binary sequence (PRBS) generator will be $1 + X^{14} + X^{15}$, as shown in Figure 11. Every data byte to be transmitted will be inserted into the randomizer sequentially, the first being Most Significant Byte (MSB). The seed value will be used to measure the randomization bits that are combined with the serialized bit stream of each burst in an XOR operation. The randomizer sequence will be used for information bits only [57].

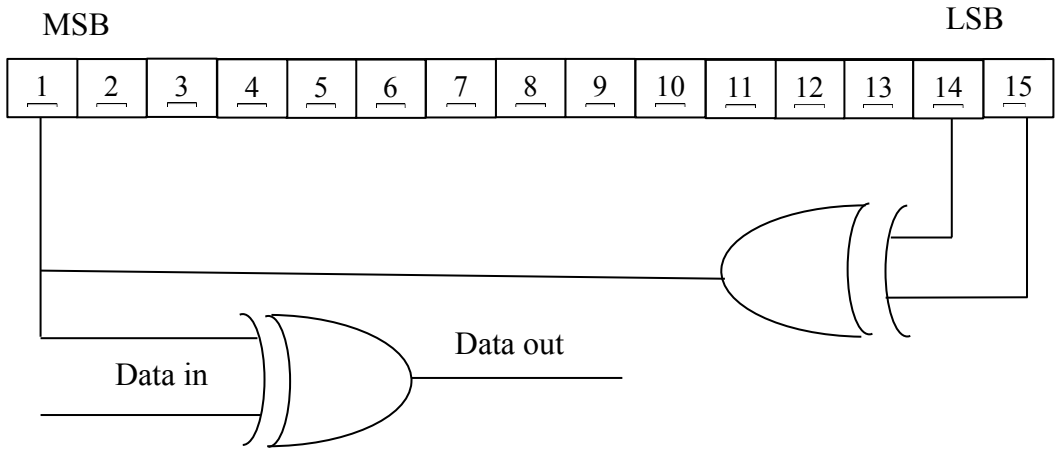

Figure 11: PRBS for data randomization

At the beginning of every frame, the randomizer is re-initialized on the downlink with the sequence 1 0 0 1 0 1 0 1 0 0 0 0 0 0 0. At the start of burst #1, the randomizer is not reset. The frame number implemented for configuration indicates the frame in that the downlink burst is transmitted [57].

4.3 Reed–Solomon Codes

Reed - Solomon codes are non - binary cyclic codes. The symbols that consist of m-bit sequences, where m is a positive integer with a value above 2. RS (n , k) codes on m-bit symbols operate for all n and k. Where n is that the total number of code symbols within the encoded block and k is that the number of data symbols being encoded.

RS codes are the largest non-binary block codes commonly used in applications. Such codes operate with symbols including several bits. The typical symbol size is a byte or eight bits for non-binary codes. RS codes are applied to correct burst errors because the correction of these codes is achieved at the symbol level. A given Reed-Solomon code is referred to by indicating it as an (n , k) code. Bose-Chaudhuri-Hocquenghem (BCH) codes are block codes that have a multiple error detection and correction capability. One of the sub-classes of BCH codes is Reed-Solomon code which is non-binary and attain the maximum (hamming) separable distance among code words for a given block size. The types of RS code most commonly used for wireless systems are systematic. The parity symbols are attached to the message symbols. The code words contain n message symbols and k parity symbols which can be used to detect and correct up to k/2 errors (if k is even). Reed-Solomon encoding is derived from a systematic RS (n = 255, k = 239, u = 8) code using GF(2^8). The parameter k refers to the number of message symbols in the code word. The parameter n refers the code word length in terms of the number of symbols in the code word. Therefore, the redundant checking part consists of n − k parity-check digits. The error correcting capability of the code is $u = \frac{(n-k)}{2}$, and minimum distance of RS code is (n-k+1) [58].

4.3.1 Reed–Solomon Encoder

A general form of the polynomial g(x) applied to generate the RS code is :-

$$g(x) = (x - \alpha^{i})(x - \alpha^{i+1}) \dots (x - \alpha^{i+2u}) \quad (4.1)$$

Where u is a number of errors which can be corrected and α is a primitive element of the "Galois field (GF)". The code word c(x) is created using:

$$c(x) = g(x)\, i(x) \quad (4.2)$$

Where the code word c(x)is exactly divisible by the generator polynomial g(x).

i(x) is the information polynomial for non-systematic encoding . For systematic encoding the remainder achieved by dividing $\mathbf{i(x)}\ \mathbf{x^{n-k}}$ / $\mathbf{g(x)}$ gives the parity polynomial $\mathbf{p(x)}$ as:

$$p(x) = \text{Rem}\frac{i(x)\, x^{n-k}}{g(x)} \tag{4.3}$$

By performing a polynomial division using GF algebra, the parity symbols are measured [59]. The stages included in this calculation are as follows:

Stage 1: Multiply the message symbols by x^{n-k} .

Stage 2: Divide the message polynomial by the code generator polynomial using GF algebra.

Stage 3: The remainder of the division is the parity symbols. In hardware, A shift register with feedback is used to achieve this. Figure 12 shows the RS encoder.

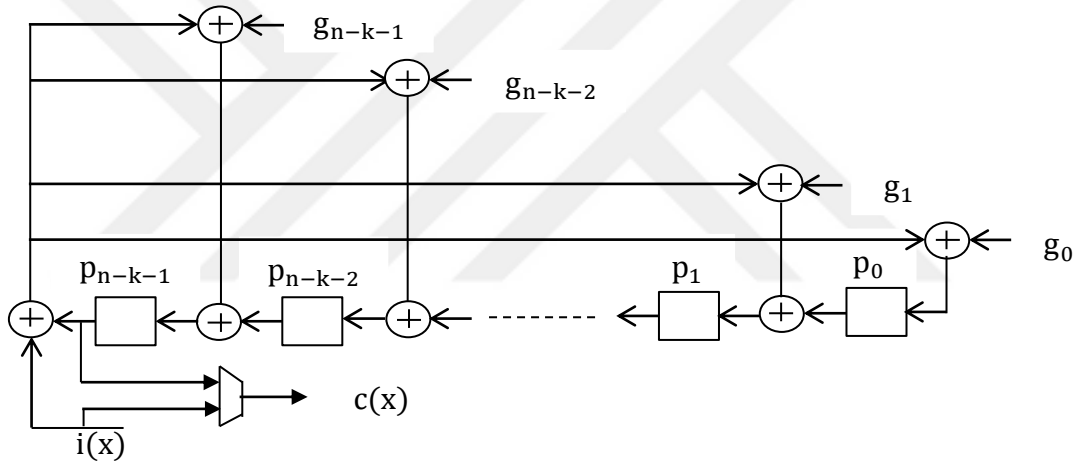

Figure 12: Reed–Solomon Encoder

where n - k represent the number of registers used.

$g_0, g_1, \ldots, g_{n-k-1}$ are coefficients of the generator polynomial g(x).

$p_0, p_1, \ldots, p_{n-k-1}$ are coefficients of the parity check symbols generated by the generator polynomial g(x).

The resultant code word systematic encoder is defined by:

$$c(x) = i(x)\, x^{n-k} + p(x) \tag{4.4}$$

4.3.2 Decoding of Reed–Solomon Codes

The Berlekamp-Massey algorithm is essential for the Reed-Solomon decoder to solve the linear equations collection. For the Reed-Solomon code an error position of u errors can be represented by error polynomial:

$$e(x) = y_{p1}x^{p1} + y_{p2}x^{p2} + \cdots + y_{py}x^{py} \quad (4.5)$$

where y_{pi} is the error magnitude at position p_i.

The Berlekamp algorithm is a quick and efficient algorithm which can find the location of an error polynomial. This algorithm is due to Massey. The Massey showed that the iterative algorithm proposed in 1967 by Berlekamp for decoding BCH codes. This algorithm can be used to find the shortest LFSR that produces a particular sequence [60].

The architecture of the RS decoder can be summarized into four steps:

1) calculating the syndromes from the received code word.
2) computing the error locator polynomial and the error evaluator polynomial.
3) finding the error locations
4) computing error values.

4.4 Convolutional Encoder

In the convolutional coding, the message bits arrive in sequentially instead of large blocks. The convolution encoder generates its coded information by converting the input message series to a set of coefficients. This group of coefficients depends on the code rate used. Using convolutional codes incessant sequence of information bits is mapped into an incessant sequence of output bits for the encoder. The encoded bits depend on current k input bits and also on past input bits [61]. The convolutional codes are presented by (n , k). where :

k is the number of input bits (uncoded).

n is number of output bits(coded).

The number of registers (D) applied during the encoding process is called the constraint length. The data rate or efficiency of a convolutional code is measured by the ratio of the number of bits in the input (k) and the number of bits in the output (n), therefore, bit rate: $r = \frac{k}{n}$. For memory elements shift register, every part holds one input bit to convolutionally encode the data. The encoder has n generator

polynomials one for every adder and mod-2 adders. The convolutional encoder (k = 1, n = 2) is shown in the Figure 13.

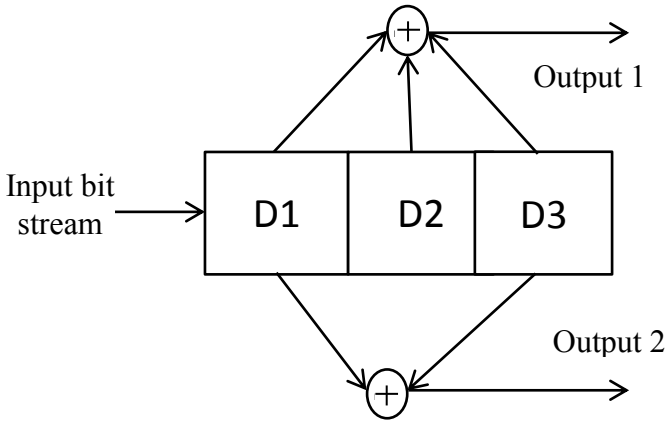

Figure 13: Convolution Encoder (k = 1, n = 2)

The selection of bits is to be added (uses XOR operation) to produce the output bits is called generator polynomial. The generator polynomials output 1 and output 2 are of (111, 101) i.e. Output 1 = mod-2 (D1 + D2+ D3), Output 2 = mod-2 (D1 + D3). If the initial contents of the register are all zeros, for the input bit stream m=0 1 1 0 1 1, the output code word sequence obtained is 11 10 10 00 10 10 11.

TABLE 1: State Table for the Convolutional Encoder (k = 1, n = 2)

Input bit m	Current State	Register Contents	Next State	Output 1	Output 2
0	00	000	00	0	0
1	00	100	10	1	1
0	01	001	00	1	1
1	01	101	10	0	0
0	10	010	01	1	0
1	10	110	11	0	1
0	11	011	01	0	1
1	11	111	11	1	0

The state table for the Convolutional Encoder (k = 1, n = 2) is shown below in Table 1. There are two alternative methods that are often used to describe a convolutional code:

a. State diagram

b. Trellis diagram

4.4.1 State Diagram

A state diagram represents the simple convolutional encoder. The status of the encoder is determined with the elements of its shift register. Every new input bit will result in the following state. There are, therefore, two possible branches for every state for one bit entered by the encoder. Two types of line are applied in order to make it easy to track the transition. Figure 14 shows every possible case of state transition for the encoder [61].

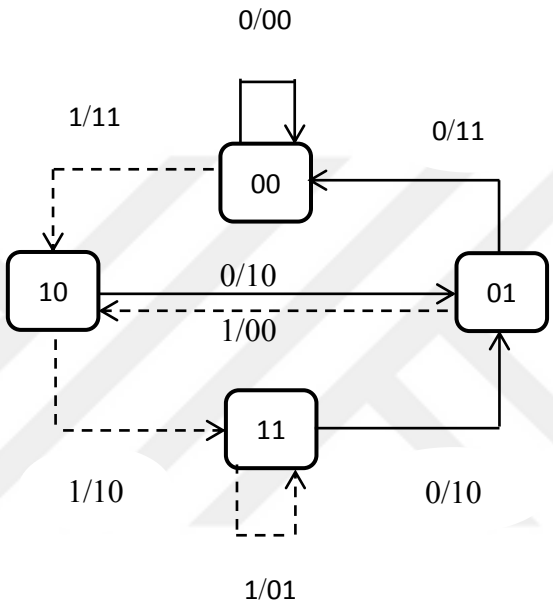

Figure 14: State Diagram (k = 1, n = 2)

4.4.2 Trellis Diagram

A trellis diagram can be used mainly for decoding of convolutional codes and is and it a kind of state diagram. The original stream detection can be defined as finding The most likely path during the trellis. In the trellis diagram, every node appoint an individual state at a given time and indicates a possible pattern of recently received data bits. Every branch indicates the transition to a new state at the next timing cycle the surviving path: When .two. paths .enter the same state, the path with the best scale is chosen. All states perform the Selection of surviving paths in the decoder. Based on the received coded bits we can choose the more likely path and ignore the least likely paths. Decoding complexity may decrease by ignoring the least likely paths.

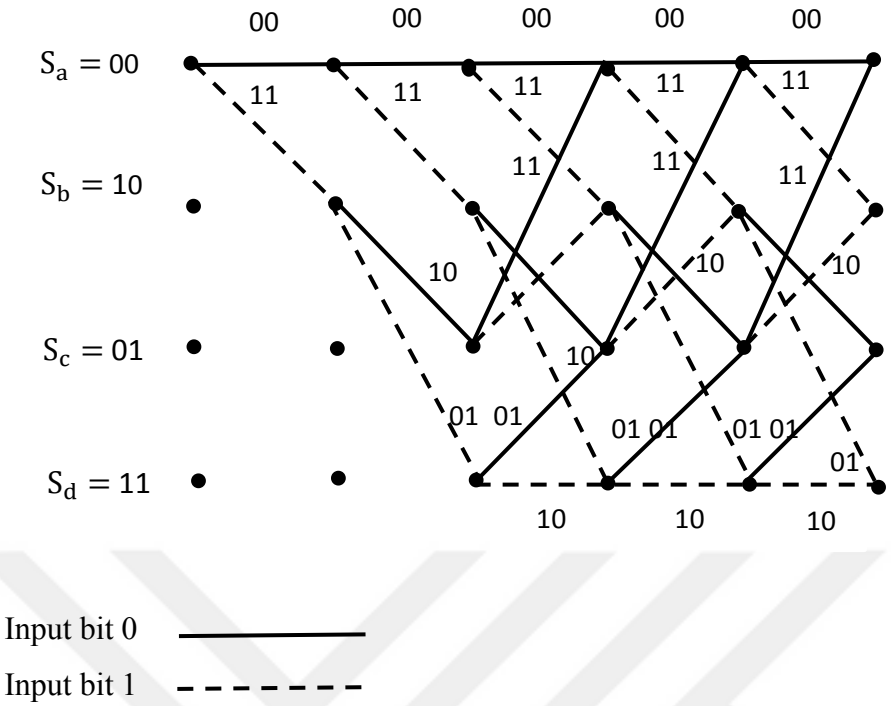

Figure 15: Encoder Trellis Structure (k = 1, n = 2)

S_a, S_b S_c and S_d are the four possible encoder states. The convolutional encoder describes the branch word that is shown on the trellis of the encoder (see Figure 15). These encoder branch words are code symbols which would have been expected to come from the output of the encoder as a consequence of the every state transition. Every part of the decoder trellis is designated with a similarity metric between the code symbol received and every of the branches for which time period as the code symbols are received. We can see here how the decoding of a surviving branch is facilitated by drawing the trellis branches with solid lines for the input 0s and dashed lines for the input 1s.

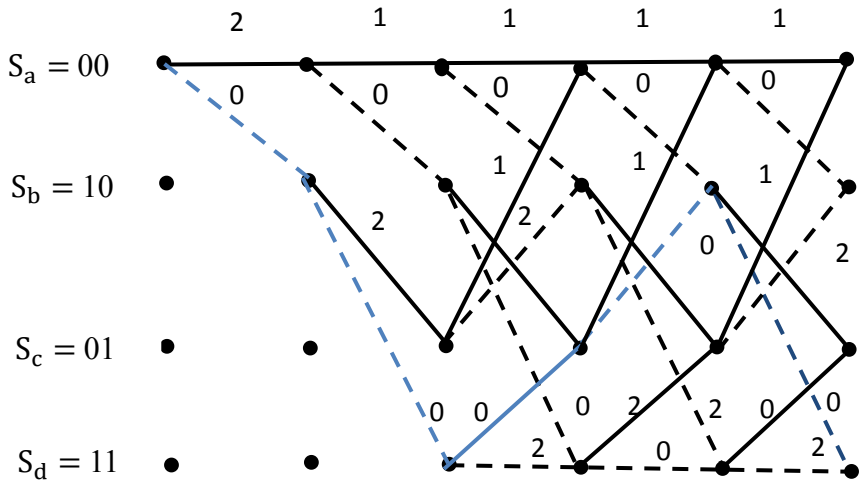

m	1	1	0	1	1
v	11	01	01	00	01
z	11	01	01	10	01

Figure 16: Structure of Decoder Trellis for (k = 1, n = 2)

In this manner, Labeling procedure is done like this. From the received sequence z, we see that the code symbol received at time t_1 is 11. In order to label the decoder branches at time t_i with the suitable Hamming distance metric presented in Figure 16. Here we see that a state 00 00 transition produces an output branch word of 00 , but we received 11.Therefore ,on the trellis of the decoder we label the stat 00 00 transition with Hamming distance among them, namely 2. Looking at the encoder trellis again ,we see that a state 00 10 transition yields an output branch word of 11,which corresponds exactly with the code symbols we received at time t_1. Therefore, on the decoder trellis, we label the stat 00 10 transition with Hamming distance 0 and so on. Thus, the metric entered on a decoder trellis branch represents the difference among what was received and what should have been received, had the branch word been associated with that branch been transmitted.

These metrics explain a correlation-like measure among every of the candidate branch words and a received branch word. We continue labeling the decoder trellis branches in this manner as the symbols are received at every time t_i. It is therefore possible to find the most likely (minimum distance) path via the trellis that would give the decoded output. At each time t_i, there are $2C - 1$ states in the trellis, where C is the constraint length, and every state can be entered by means of two ways. Viterbi decoding consists of calculating the metrics for the two paths which are

entering every state and eliminating one of them. This calculation is performed for every one of the 2C − 1 states or nodes at time t_i, followed by the decoder moving to time $t_{(i+1)}$ and repeating the process. At a given time, the state metric for the winning path metric for each state is determined at that time. Figure 16 presents the state metric comparison at every state and the decoding process uninterrupted for all the state transitions in order to make decisions on the input data bits by eliminating all paths but one. In the decoding process at time t_1, the received code symbols are 11. The only transitions from state 00 are to state 00 or 10. The state 00 to 00 transition has a branch metric of 2 and the state 00 to 10 transition has a branch metric of 0. At time t_2, there are two possible parts leaving every state metric $S_a = 2$ and $S_b = 0$, as shown in Figure 16. Likewise, the same process will continue for all other states, the state metric S_d=1 is the maximum likelihood and the path metric branch word sequence is 11 01 01 10 01.

4.4.3 The Viterbi Convolutional Decoder

The Viterbi decoder can be divided into in three steps:

Step 1: Determine the Hamming distance of each path.
Step 2: Add the distance of each path.
Step 3: Compare and select the shortest path.

The Viterbi decoding algorithm was discovered and analyzed by Viterbi in 1967. Viterbi algorithm essentially performs maximum likelihood decoding; however, it reduces the computational load by taking advantage of the special structure in the code trellis. In comparison with brute force decoding, the benefit of Viterbi decoding is that the complexity of a Viterbi decoder does not depend on the number of symbols in the code word sequence. The algorithm contains calculating similarity measure among the signal gained at the time and all the paths of the trellis entering every state at the time. The Viterbi algorithm excludes those paths of the trellis, which could not be a candidate for the maximum likelihood choice. If two routes arrive in the same state, the one having the best metric is selected and is called the surviving path. For all states, this selection of surviving paths is done for all states. In this manner, the decoder continues to advance deeper into the trellis, making choices by removing the least likely path. The goal of selecting the optimal path can be represented equally as

selecting the code word with the maximum likelihood metric or the d_{min} metric [61]. The poly2trellis(7, [171 133]) notation shows a trellis form for a binary convolutional code with constraint length 7 and feedback taps placed at the octal numbers 171 (binary 1111001) and 133 (binary 1011011). Figure 17 shows convolutional encoder with code rate 1/2 for the poly2trellis(7, [171 133]) structure. There are six delay elements denoted by z - 1 in the encoder with the constraint length 7 corresponding to the number of bits stored in the shift register. The free distance d_{free} of the convolutional code is d_{min} in the set of all arbitrarily long paths that diverge from the all-zero state and re-enter the all-zeros state. The number of errors u that can be corrected by the code is given by:

$$u = \left\lfloor \frac{d_{free} - 1}{2} \right\rfloor \tag{4.6}$$

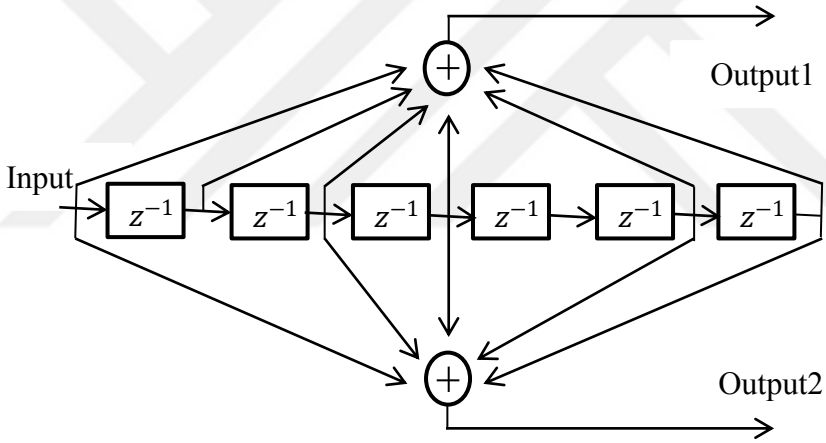

Figure 17: Convolutional Encoder with Code Rate 1/2

4.5 Interleaver

Interleaving can be used to minimize the impact of burst errors in digital data transmission technologies. When too many errors exist in one code word, due to a burst error, the decoding of a code word cannot be done correctly. The bits in a single code word are interleaved before being transmitted to decrease the impact of a burst error. The place of bits varies as interleaving happens, which ensures that a burst error does not disturb a significant part of a code word [58]. A block interleaver must interleave all encoded data bits with a block size equivalent to the number of coded bits per the encoded N_{cbps} block size. The interleaver shall be based on a two-

step permutation. The first step ensures that adjacent coded bits are mapped onto non-adjacent sub-carriers and the second step insures that adjacent coded bits are mapped alternately onto fewer or more significant bits of the constellation, thus avoiding long runs of low-reliability bits. Where : j_k is the index after the second permutation just prior to modulation

mapping.

k is the index of the coded bit before the first permutation.

m_k is the index after the first permutation and before the second permutation.

Let N_{cbps} is the block size corresponding to the number of coded bits per allocated sub-channels per OFDM, N_{cpc} is the number of coded bits per subcarrier and s = ceil $\left(\frac{N_{cpc}}{2}\right)$. The first permutation is specified by the rule:

$$m_k = \left(\frac{N_{cbps}}{12}\right).k_{mod12} + floor\left(\frac{k}{12}\right) \qquad k = 0,1,\dots,N_{cbps}-1 \qquad (4.7)$$

where k is the index of the coded bit before the first permutation

The second permutation is specified by the rule:

$$j_k = s\,.floor\left(\frac{m_k}{s}\right) + \left(m_k + N_{cbps} - floor\left(\frac{12\,.\,m_k}{N_{cbps}}\right)\right)_{mod\,(s)} \qquad k = 0\,,1,\dots,N_{cbps}-1 \qquad (4.8)$$

Two permutations also describe the de-interleaver, which implements the inverse relation. We shall point to :-

j is the index of the original received bit before the first permutation,

m_j is the index after the first and before the second permutation,

k_j is the index after the second permutation,

just prior to delivering the coded bits to the convolutional (Viterbi) decoder.

The first permutation is performed as :

$$m_j = s\,.floor\left(\frac{j}{s}\right) + \left(j + floor\left(\frac{12.j}{N_{cbps}}\right)\right)_{mod(s)} \qquad j = 0,1,\dots,N_{cbps}-1 \qquad (4.9)$$

The second permutation is performed as :

$$k_j = 12\,.\,m_j - \left(N_{cbps}-1\right).floor\left(\frac{12\,.\,m_j}{N_{cbps}}\right) \qquad j = 0,1,\dots,N_{cbps}-1 \qquad (4.10)$$

4.6 Data modulation

The data bits are entered serially in the constellation mapper. Figure 18 shows QPSK, 16-QAM and 64-QAM constellations. The constellations are normalized by multiplying the constellation point with the factor to achieve equal average power. For every modulation, b_0 denotes the Least Significant Byte (LSB).

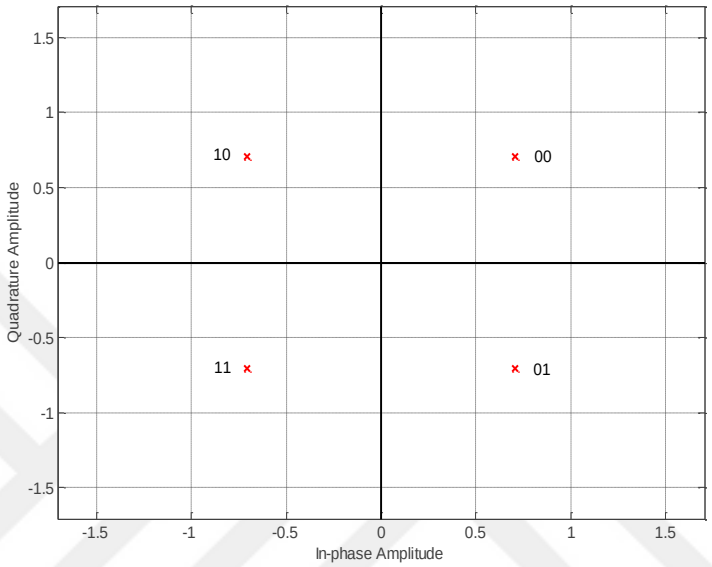

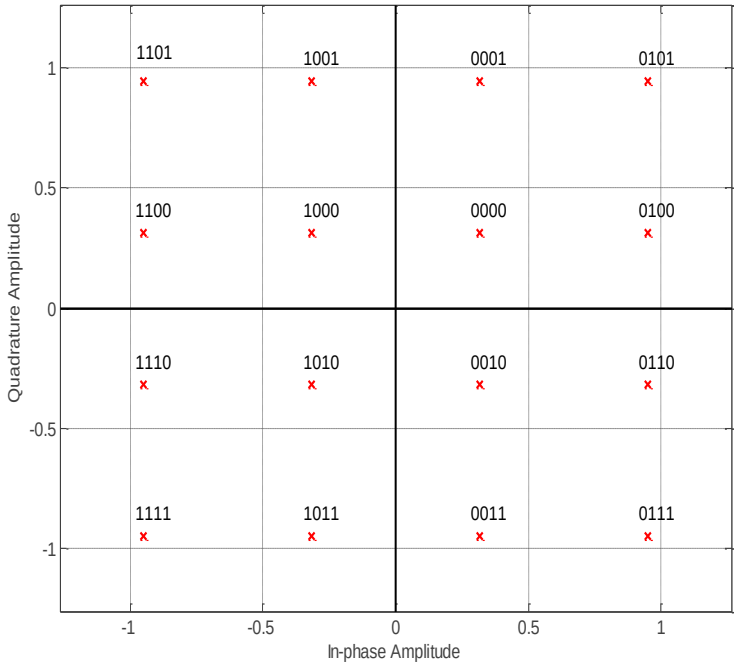

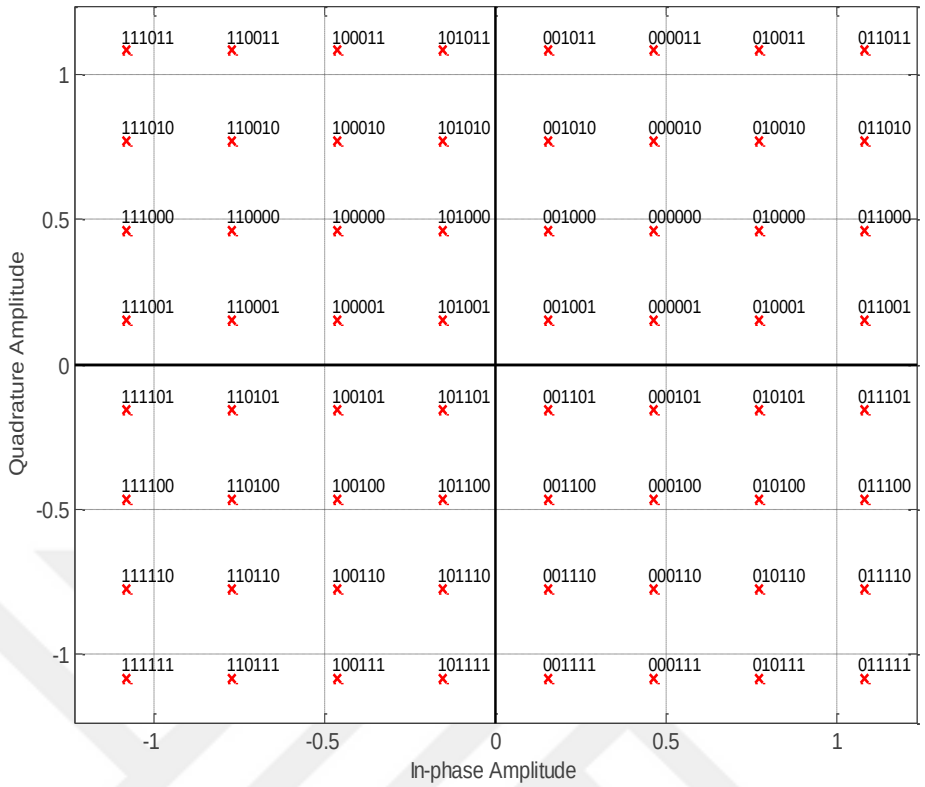

Figure 18: QPSK, 16-QAM, and 64-QAM Constellations

4.7 MIMO-OFDM Signal Model

We consider a MIMO-OFDM system where the space-time processing technique of MIMO is implemented, then encoding can be carried out collectively over the multiple transmitter antennas or an individual antenna. Encoding that occurs on an individual antenna is called per antenna coding (PAC) [62].

4.7.1 Transmitter Tx

For the number of transmit antennas equal to N_t , there would be N parallel branches of the OFDM technique or N_t OFDM transmitters. Every branch in parallel performs the same transmission process for the input binary data. Firstly for each parallel bit stream coding, interleaving and modulation (16-QAM) are performed. Then in accordance with the pilot patterns, pilot symbols are added. Subsequently, the symbol sequence in frequency is modulated by IFFT in an OFDM and the cyclic prefix (CP) is added to every OFDM symbol. Finally, the signal is transformed to radio frequency elements for transmission [62].

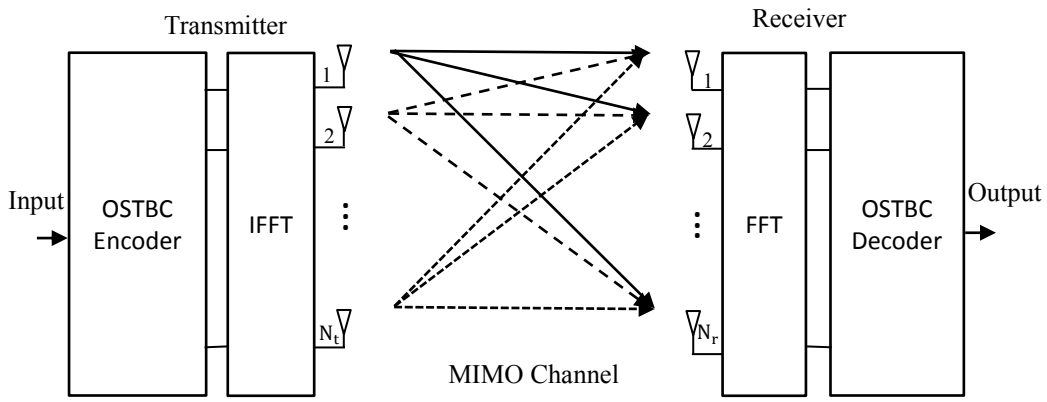

Figure 19: Basic Block Structure of MIMO-OFDM System

Figure 19 shows the basic block structure of MIMO-OFDM system, which is the dominant air interface for 4G and 5G broadband wireless communications. It combines multiple input and multiple output (MIMO) technology and multiplies capacity by transmitting different signals over multiple antennas and orthogonal frequency division multiplexing (OFDM).

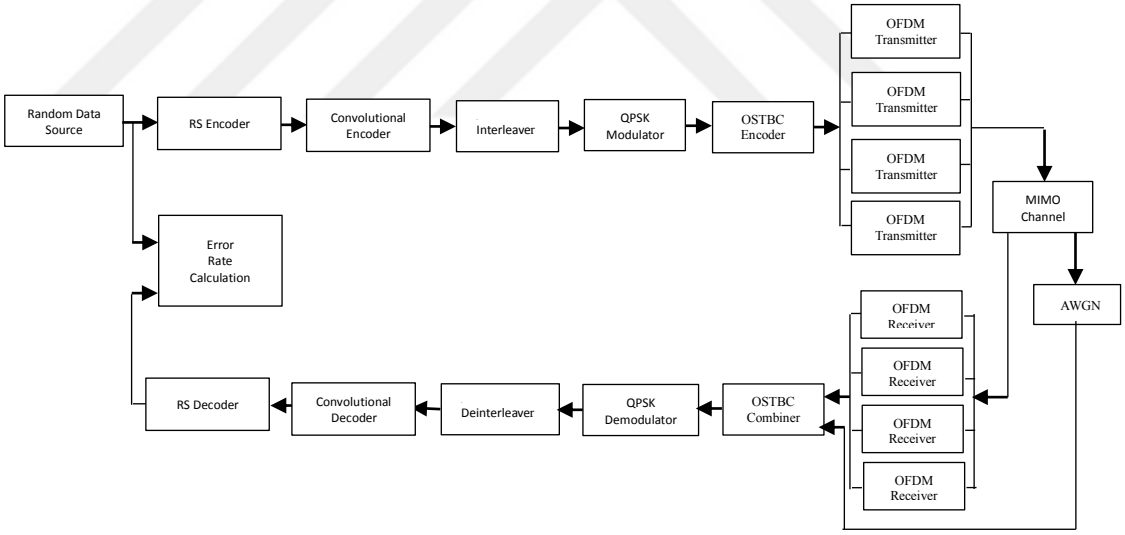

Figure 20: Basic Block Structure of RS-CC Codes with MIMO-OFDM

Figure 20 shows the basic block structure of the Convolutional Code and the Reed-Solomon code with the MIMO-OFDM system. The RC-CC codes are a concatenated code of Reed-Solomon code as the inner code and Convolutional Code as the outer code.

4.7.2 Receiver R_X

For the number of transmit antennas equal to N_r, there will be N_r OFDM receivers. The symbol received from the radio-frequency element is first synchronized (frequency and time). Subsequently, the cyclic prefix is extracted from every stream of receiver symbols and the OFDM symbols in every branch are then demodulated by FFT. Pilot symbols are removed as a subsequent step, followed by demodulation, decoding and de-interleaving. Finally, the binary output data is the resulting data after combining.

4.7.3 Frame Structure

The MIMO-OFDM frame structure is a small transmission unit with ten slots in the time domain. Each slot contains eight symbols and one preamble slot. The MIMO-OFDM System Frame Structure is shown in Figure 21.

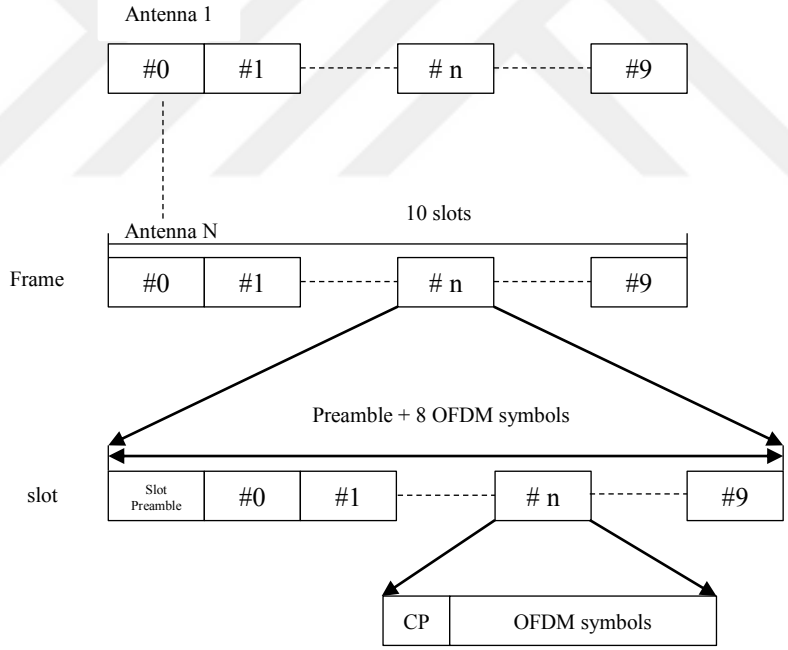

Figure 21: MIMO-OFDM System Frame Structure.

Preamble is applied for each OFDM slot containing the cyclic prefix to reduce the effect of ISI and for the synchronization of time. The arrangement among the data to be transmitted to the sub-carriers and the components of the frame contains pilot symbols. Timing estimates can be used in pilot symbols when synchronization is completed.

4.7.4 MIMO-OFDM advantages

- ⇨ Bandwidth gain.
- ⇨ Fewer occurrences of infringement.
- ⇨ Power efficiency.
- ⇨ Data capacity enhancement.
- ⇨ Diversity gain.

CHAPTER 5

PERFORMANCE ANALYSIS

5.1 Simulation Program Description

The main components of the MIMO-OFDM physical layer are presented using OSTBC by describing the tasks performed during the communication scheme model. These consist of:

Random bit data generated which representations a downlink burst containing an integer number of OFDM symbols. FEC, which includes an outer Reed-Solomon (RS) code linked to a rate-compatible inner convolutional code (CC). Data interleaving: The Matrix Interleaver block implements block interleaving by filling a matrix with the input symbols row by row and then sends the matrix contents to the output port column by column. Modulation using the specified QPSK, 16-QAM or 64-QAM constellations. OFDM transmission using 192 sub-carriers, 8 pilots, 256-point FFTs, and a 0.125 cyclic prefix length. Alamouti code is one of the types of space-time block code. The OSTBC Encoder and Combiner blocks in the wireless communication system are used in this implementation. The OSTBC Encoder object encodes an input symbol sequence using Orthogonal Space-Time Block Code (OSTBC). The block maps the input symbols block-wise and concatenates the output code word matrices in the time domain. The OSTBC Combiner block combines the input signal (from every receive antenna) and the channel estimate signal to extract the soft information of the symbols encoded by an OSTBC. OSTBCs are an attractive technique for MIMO wireless communications. It uses symbol-wise maximum likelihood (ML) decoding and uses the complete order of spatial diversity. The four transmitted signals from the OSTBC encoder pass through the 4 × 4 MIMO Rayleigh fading channel or Rician fading channel and are also impaired by AWGN. The AWGN Channel block adds white Gaussian noises at the receiver side. The Mode parameter is set to the Signal-to-Noise Ratio (SNR) mode and the Input signal power is referenced to 1 ohm (watts). The OSTBC Encoder and combiner blocks in

the Communications Blockset are used in this implementation. A single OFDM symbol length preamble is applied as the burst preamble. In the OSTBC system, each antenna transmits the single symbol preamble. In the OSTBC method, this indicates combining diversity followed by Hard-decision demodulation, de-interleaving, Viterbi decoding and Reed-Solomon decoding.

5.2 Design methodology

The block diagram in Figure 22 shows the steps to be performed. Explanations for each step are given below:

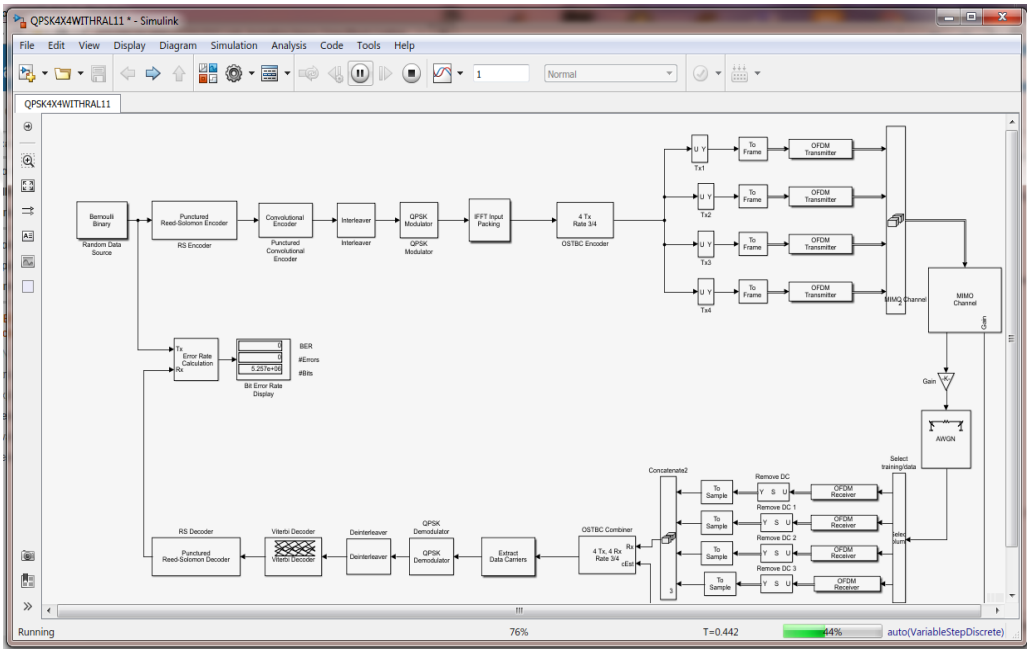

Figure 22: MIMO_OFDM using OSTBC with Forward Error Correction

- Randomization is the first process carried out in the layer after the data packet is received from the higher layers. Every burst in Downlink and Uplink is randomized. It basically scrambles data to generate random sequences to improve coding performance.

- Forward Error Correction (FEC) uses a number of coding systems, such as RS codes, convolution codes, Turbo codes, etc. However, in the present work, only RS codes, Convolution Codes and Interleaver were used in the simulation. The RS codes add redundancy to the data. This redundancy improves Block's error. The RS encoder is based on Galois field computation to add redundancy bits.

- Interleaving aims to distribute transmitted bits in time or frequency, or both, to achieve desirable bit error distribution after demodulation. The desirable error distribution depends on the used FEC code and the required interleaving pattern depends on the channel characteristics.

- Modulation and channel coding are fundamental components of a digital communication system. Modulation is the process of mapping digital information to analog form so it can be transmitted over the channel. Consequently, every digital communication system has a modulator that performs this task. Closely related to modulation is the inverse process, called demodulation, which is performed by the receiver to recover the transmitted digital information.

- An inverse Fourier transform converts the frequency domain of data input to the time domain describing the OFDM sub-carrier. IFFT is useful for OFDM because it produces frequency component samples of a waveform that satisfy the condition of orthogonality.

In this thesis, the effects of increasing the order of modulation on BER performance of the system are presented for various MIMO configurations the behavior of the MIMO(OSTBC)-OFDM system in various environments is studied and the effects of increasing the order of modulation on BER performance of the system are presented for various MIMO configurations. These Specifications of MIMO-OFDM using OSTBC are given in Table 2.

Table 2: Simulation Parameters

Parameters	Values
FFT Size	256
No. of used sub-carriers	192
Ratio guard time to symbol time(G)	0.1250
Convolutional Code	poly2trellis (7, [171 133])
Code Rate of OSTBC	3/4
SNR Range	0-50 dB
Modulation	QPSK, 16-QAM, 64-QAM
Channel Model	Rayleigh channel - Rician channel
Configuration antennas	1 × 1, 2 × 2, 3 × 3 and 4 × 4

The system discussed above has been designed using the OSTBC code structure for the MIMO-OFDM method. For different modulations and different channels, the results are shown in the form of the BER vs. SNR plot. Here, various antenna configurations such as 1 × 1, 2 × 2, 3 × 3 and, 4 × 4 antenna configurations are used. Analyses are made for different wireless fading channels, the namely Rician and Rayleigh channels with the results being presented for different antenna configurations over different MIMO fading channels using QPSK, 16-QAM and 64-QAM.

5.3 BER Results of MIMO-OSTBC system

In this section, BER analysis of the MIMO-OSTBC system using QPSK over different fading channels is presented. First, an analysis of the MIMO-OSTBC system using QPSK is presented over the Rayleigh and Rician channels.

5.3.1 Different Antenna Configurations for MIMO-OSTBC System over Rayleigh Fading MIMO Channel.

In this section, the performance of Orthogonal Space Time Block Coding (OSTBC) Multiple Input Multiple Output (MIMO) systems using FEC codes (Reed-Solomon, Convolutional and Interleaving) are used to encode the data stream in wireless communications through the Rayleigh channel. These are subjected to experimentation under modulation techniques, such as Quadrature Phase Shift Keying (QPSK). MIMO systems with multiple antenna elements at the ends of transmitters and receivers are efficient solutions for wireless communication systems [63]. Decoding is carried out using the Maximum Likelihood (ML) algorithm. The block diagram of the MIMO-OSTBC system is shown in Figure 23.

MIMO systems provide high data rates using spatial domains under the limits of bandwidth and power transmission. Various simulations are performed to detect the best BER performance of the different values of antenna configurations with FEC codes and to use the best outcomes to model the OSTBC. Their effect of improving the overall BER can be noticed with the benefits of OSTBC with FEC codes and the maximum number of configurations [63].

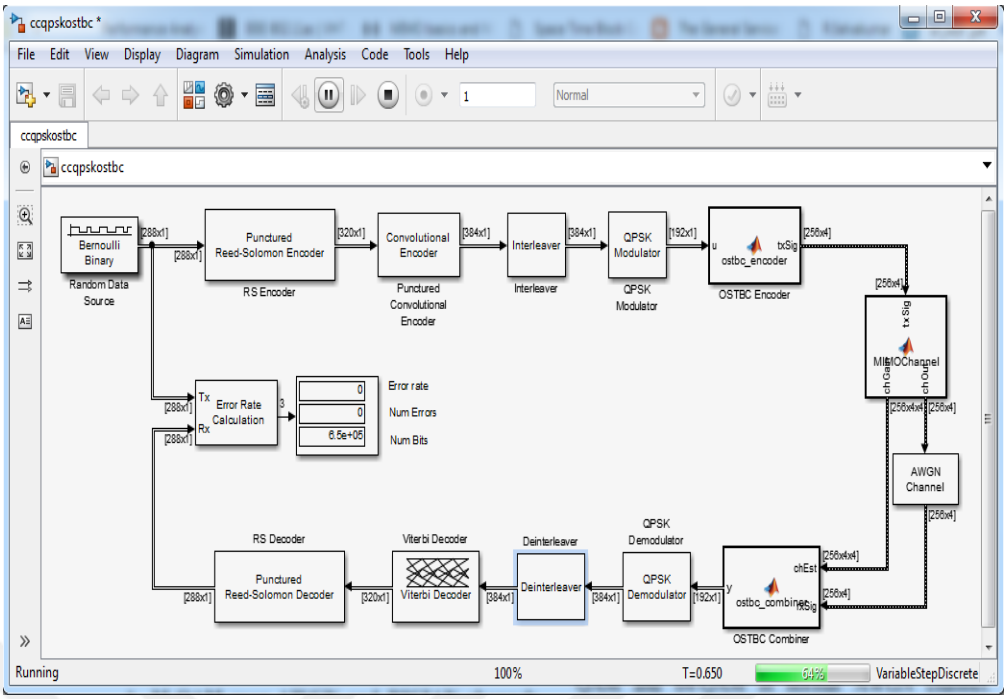

Figure 23: MIMO-OSTBC System with FECs

5.3.1.1 BER Results of MIMO-OSTBC system without channel coding.

In this section, BER analysis of MIMO-OSTBC systems using QPSK and the Rayleigh fading channel without FECs is presented.

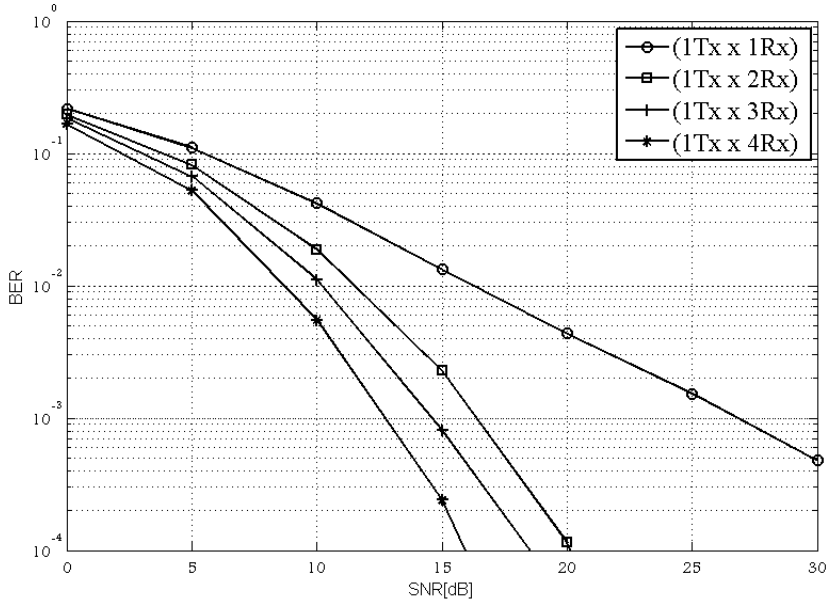

Figure 24: BER vs SNR plots for MIMO-OSTBC Performance in QPSK Without Channel Coding for Tx=1.

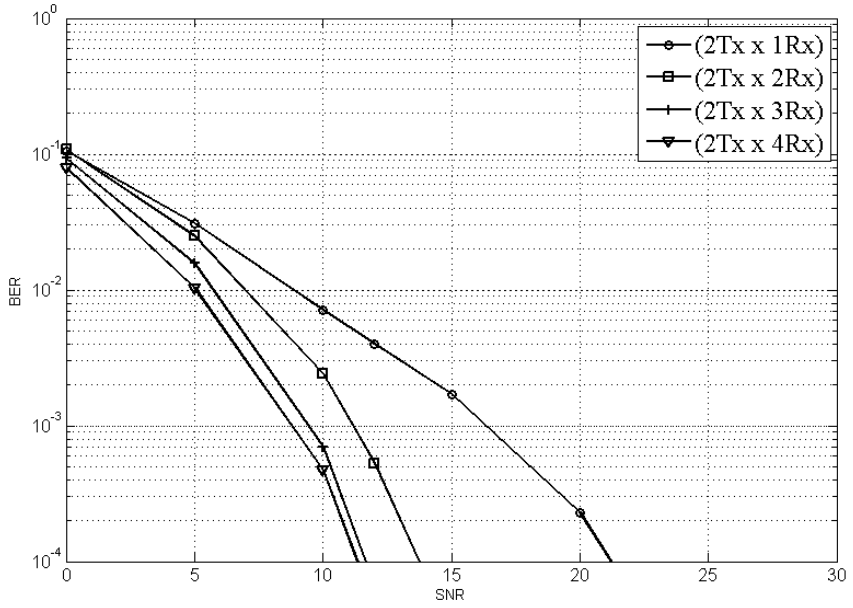

Figure 25: BER vs SNR Plots for MIMO-OSTBC Performance in QPSK Without Channel Coding for Tx=2.

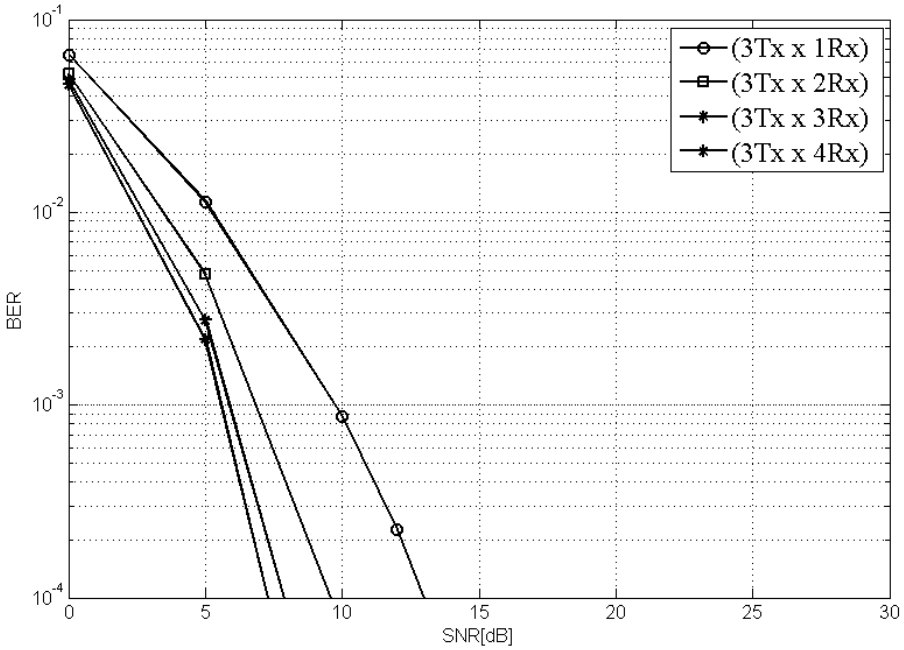

Figure 26: BER vs SNR Plots for MIMO-OSTBC Performance in QPSK Without Channel Coding for Tx=3.

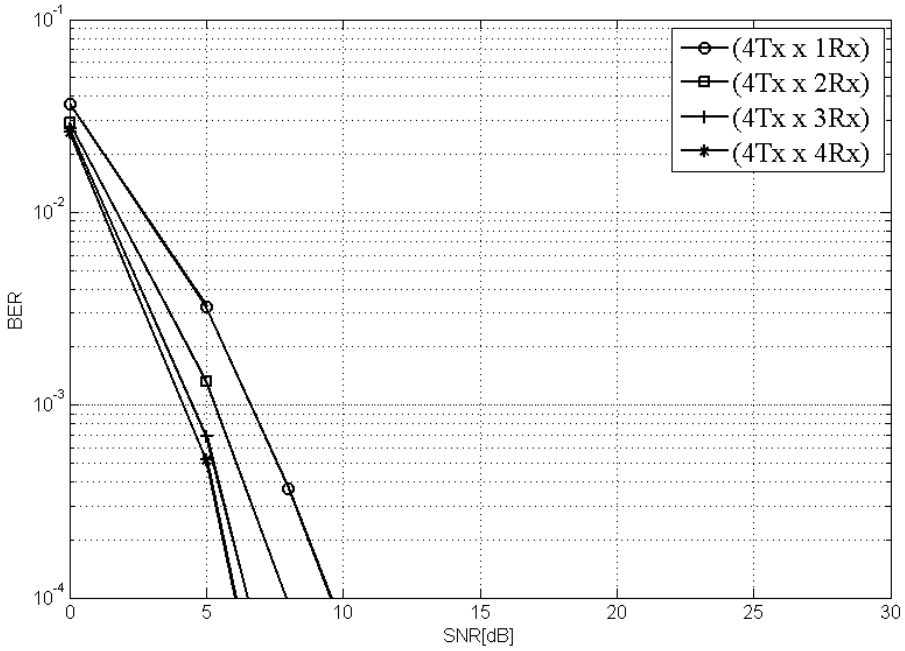

Figure 27: BER vs SNR Plots for MIMO-OSTBC Performance in QPSK Without Channel Coding for Tx=4.

For the MIMO-OSTBC technique, SNR vs. BER plots using QPSK over the Rayleigh fading channel employing various antenna configurations are shown in Figures 24, 25, 26 and 27. The graphs clearly offer the impression that as we continue to increase the number of transmitting and receiving antennas in the MIMO-OSTBC method and due to space diversity, the BER continues to decrease. The proposed scheme offers much better BER efficiency compared to other antenna configurations [63].

The prevalence of using higher order 4 × 4 antenna configurations over lower order 1 × 1 antenna configurations is shown in the form of SNR gain in dB for QPSK over the Rayleigh fading channel. As we move on with higher order antenna configurations, the BER will continue to decrease. Table 3 shows the improvement in the MIMO-OSTBC system using QPSK modulation and the Rayleigh fading channel without FECs.

Table 3 Improvement for MIMO-OSTBC system using QPSK modulation and Rayleigh fading channel without FECs.

Number of transmitting antennas and receiving antennas	SNR when BER $= 10^{-3}$ in dB	SNR when BER $=10^{-4}$ In dB
1 × 1	27	35
1 × 2	16.5	20.5
1 × 3	14.5	19
1 × 4	12.8	16.8
2 × 1	16.5	22
2 × 2	11.5	14
2 × 3	9.5	12
2 × 4	9	11.8
3 × 1	9.8	15
3 × 2	6.9	9.6
3 × 3	5.9	7.9
3 × 4	5.5	7.2
4 × 1	6.8	9.5
4 × 2	5.2	7.9
4 × 3	4.5	6.5
4 × 4	4.2	6.1

5.3.1.2 BER Results of MIMO-OSTBC system with channel coding.

In this section, BER analyses of the MIMO-OSTBC technique using QPSK modulation and the Rayleigh fading channel with FECs are presented.

From Figures 28, 29, 30 and 31, it is clear that the performance of the Reed-Solomon, Convolutional and Interleaving systems concatenated code outperform non-concatenated codes. It can be seen that RSC-CC and the Interleaving curve show a lower flattening effect with a much better slope than the others without channel codes. It is cleared that the BER with coding outperformed BER without coding.

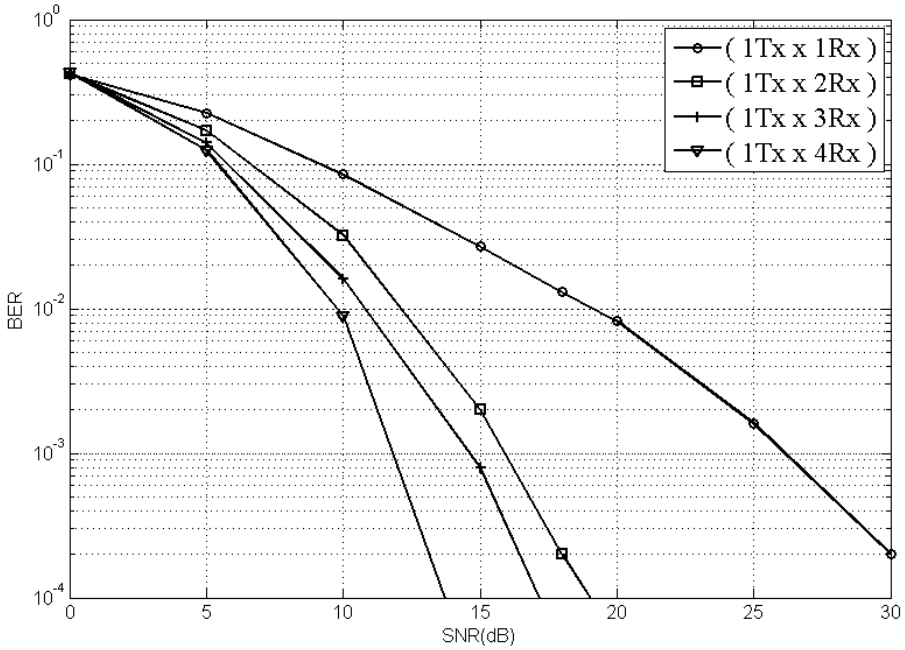

Figure 28: BER vs SNR Plots for MIMO-OSTBC Performance in QPSK With Channel Coding for Tx=1.

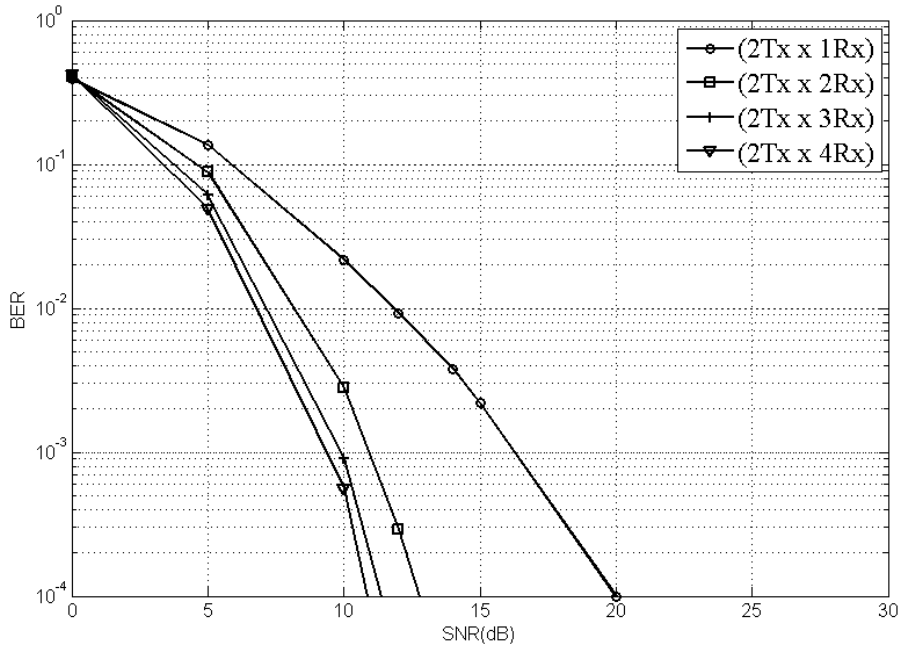

Figure 29: BER vs SNR Plots for MIMO- OSTBC Performance in QPSK With Channel Coding for Tx=2.

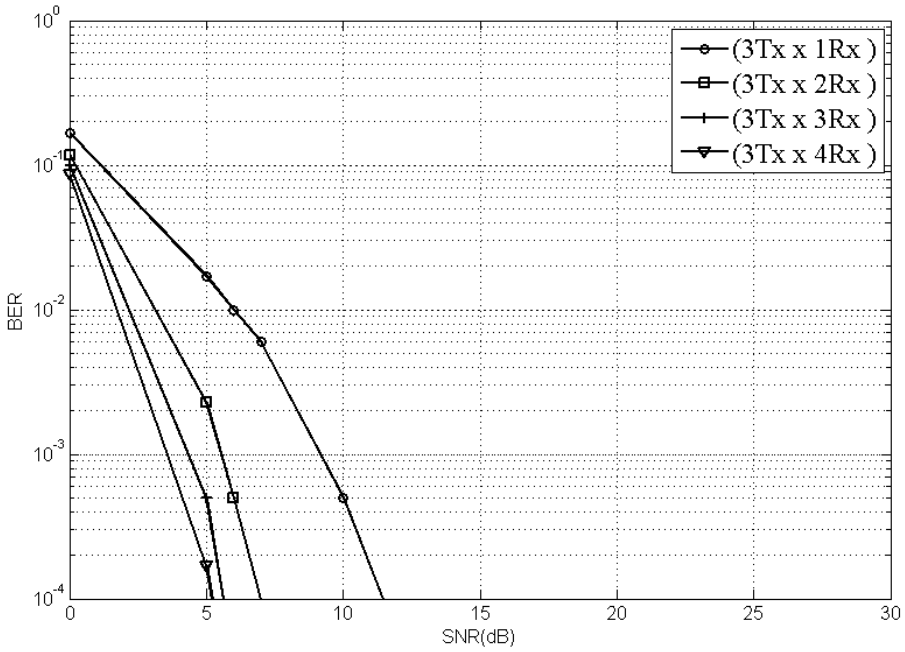

Figure 30: BER vs SNR Plots for MIMO-OSTBC Performance in QPSK With Channel Coding for Tx=3.

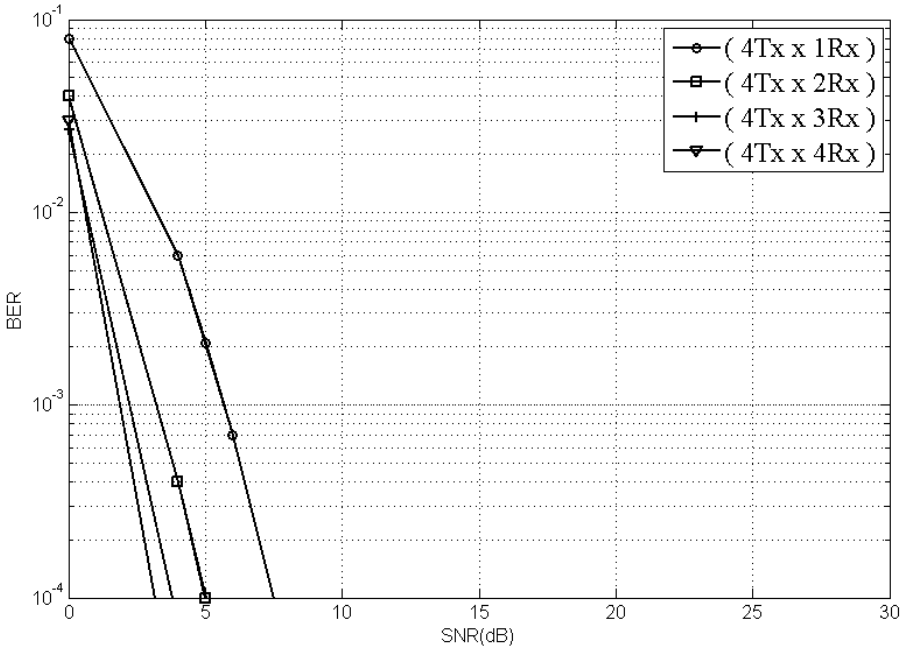

Figure 31: BER vs SNR Plots for MIMO-OSTBC Performance in QPSK With Channel Coding for Tx=4.

For OSTBC with 4 × 4 antenna configuration and QPSK, the SNR value needed to attain a BER of 10^{-3} is 4.2 dB and for a BER of 10^{-4}, it is 6.1 dB. The corresponding SNR values of the OSTBC with FECs are 1.8 dB and 3.2 dB. The improvement in the performance of the BER of OSTBC with FECs is better than in the same system without FECs. Table 4 shows the improvement for MIMO-OSTBC system using QPSK modulation and Rayleigh fading channel with FECs.

Table 4 Improvement for MIMO-OSTBC system using QPSK modulation and Rayleigh fading channel with FECs.

Number of transmitting antennas and receiving antennas	SNR when BER $=10^{-3}$ in dB	SNR when BER $=10^{-4}$ In dB
1 × 1	26	32
1 × 2	16	18
1 × 3	14.5	17.5
1 × 4	11.5	14.1
2 × 1	16.5	20
2 × 2	11	12.4
2 × 3	10	11.5
2 × 4	9.5	11
3 × 1	9	11.5
3 × 2	5.5	7
3 × 3	4.3	5.5
3 × 4	3.5	5.2
4 × 1	5.3	7.5
4 × 2	3.2	5
4 × 3	2.3	3.8
4 × 4	1.8	3.2

5.3.2 Different Antenna Configurations for MIMO - OSTBC System Using channel coding and Rician Fading MIMO Channel.

In this section, an analyses and simulations of the Multiple-Input Multiple-Output (MIMO) system with the Quadrature Phase Shift Keying (QPSK) are performed using Orthogonal Space Time Block Coding (OSTBC). Unlike traditional

methods that use only the time dimension, OSTBC uses the time and spatial dimensions simultaneously for error control. This section simulates the MIMO-OSTBC system with one, two, three or four transmit or receive antennas, i.e., 1×1, 2×2, 3×3 and 4×4. The modulation employed is QPSK, while the channel model can be Rician fading type error correction schemes such as Reed-Solomon Code (RSC), Convolutional Code (CC) and Interleaving. MIMO is analyzed and simulated using OSTBC with QPSK with different antenna configurations. A comparative study shows that the performance of MIMO using OSTBC with QPSK improves for high order antenna configurations for given channel conditions and data rates. Such a performance improvement inevitably leads to lower BER. The MIMO technique is applied with different antenna configurations such as 2×2 using orthogonal space-time block coding. The system is simulated for BER performance using the QPSK modulation technique under the same channel conditions with different SNR values and different antenna configurations.

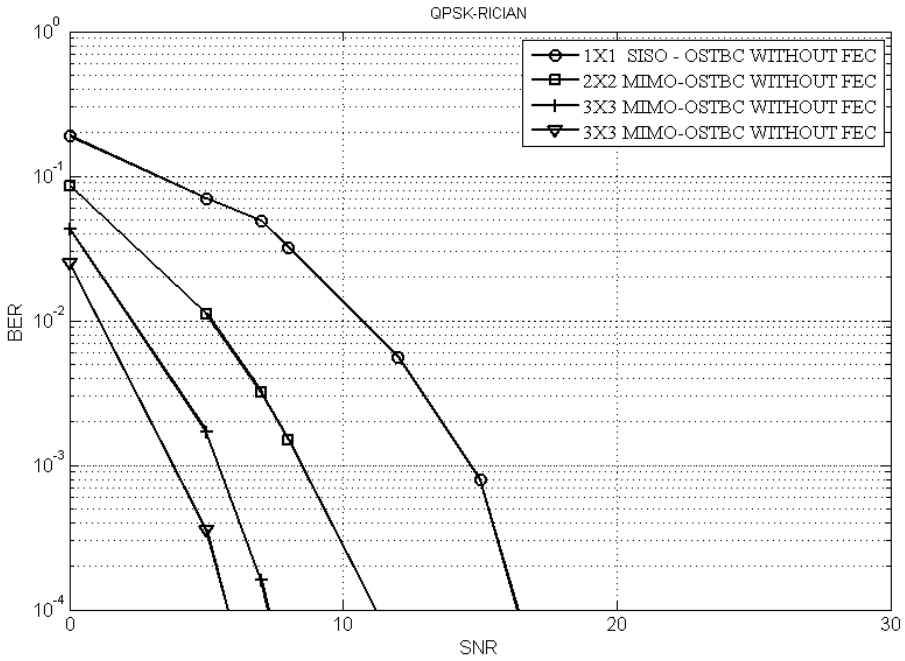

Figure 32: BER of MIMO-OSTBC for QPSK Modulation Techniques Without Channel Coding .

The plot of SNR against BER is obtained for systems using 1×1, 2×2, 3×3 and 4×4, as shown in Figure 32. The system QPSK modulation without FEC is further analyzed and simulated for different antenna configurations. The parameters that are used for the simulations are listed in Table 5. It is observed that the performance of

the MIMO-OSTBC system improves with an increase in SNR for the QPSK modulation scheme with maximum antenna configuration.

Table 5 List of Simulation parameters.

System parameters	Specifications
Channel model	Rician
K factor	4
Modulation	QPSK
No. of Transmitting and receiving antennas	1 × 1, 2 × 2, 3 × 3 and 4 × 4

Figure 32 shows the simulation results of the BER analysis of QPSK modulation for Rician fading channel without channel coding.

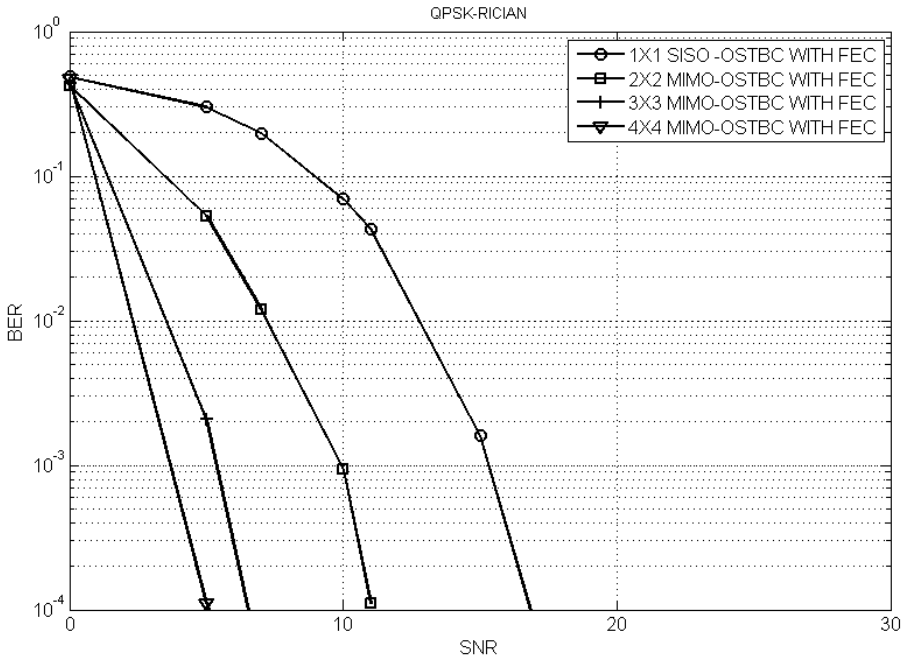

Figure 33: BER of MIMO-OSTBC for QPSK Modulation Techniques With Channel Coding .

A simulation is performed for the QPSK modulation method. The graphs show that 4 × 4 is better than 3 × 3, 2 × 2 and 1 × 1. If two transmitting antennas (i.e., 2 × 2) are replaced by four transmitting antennas (i.e., 4 × 4), then the overall performance of the system improves.

Figure 33 shows that a 4 × 4 configuration is better than a 3 × 3 configuration. If three transmitting antennas 3 × 3 are replaced by four transmitting antennas 4 × 4, then the overall performance of the system improves.

Table 6 Improvement for MIMO-OSTBC system using QPSK modulation and Rician fading mimo channel with FECs.

Number of transmitting antennas and receiving antennas	SNR when BER=10^{-3} in dB	SNR when BER=10^{-4} In dB
1× 1	4.1	5.2
2× 2	6	7.6
3× 3	10	11.5
4× 4	15.1	17.3

Simulation is performed for the QPSK modulation method. Table 6 shows that QPSK performs better when we use a higher order antenna configuration with FEC. The results above show that the system exhibits better results with QPSK and 4 × 4 when compared with other antenna configurations.

5.3.3 Study of Different Antenna Configurations for MIMO-OFDM using OSTBC system over Rayleigh Fading MIMO Channel.

5.3.3.1. MIMO(OSTBC) - OFDM Technique over Rayleigh MIMO Fading Channel without Using FECs.

In this section, the study presents the system performance by calculating the Bit Error Rate with different values of the Signal-to-Noise Ratio. The aim of this work is to investigate deeply the behavior of a MIMO-OFDM using the Rayleigh fading channel with different modulation techniques, such as QPSK, 16-QAM and 64-QAM, without channel coding. The MIMO(OSTBC)-OFDM system here contains a data source, a QPSK, 16-QAM or 64-QAM modulator, an OSTBC encoder and OFDM at the transmitter. The BER results obtained using the simulation are presented in Figures 34, 35 and 36, which show the performance of 1 × 1, 2 × 2, 3 × 3 and 4 × 4 MIMO(OSTBC)-OFDM, respectively for QPSK, 16-QAM and 64-QAM over the Rayleigh channel without FECs.

.

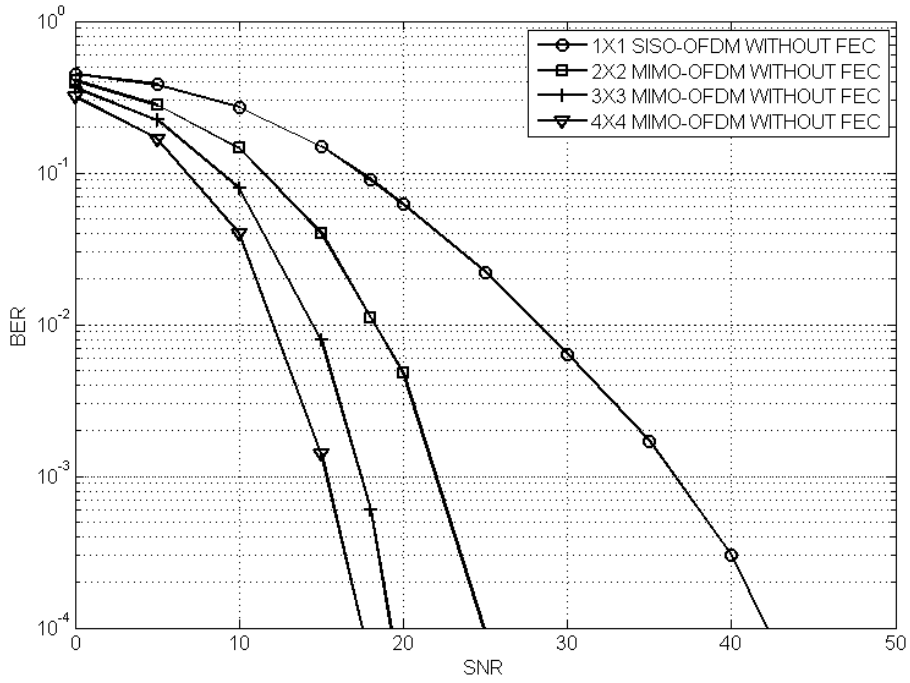

Figure 34: BER vs SNR Plots for QPSK over Rayleigh Channel Without FECs

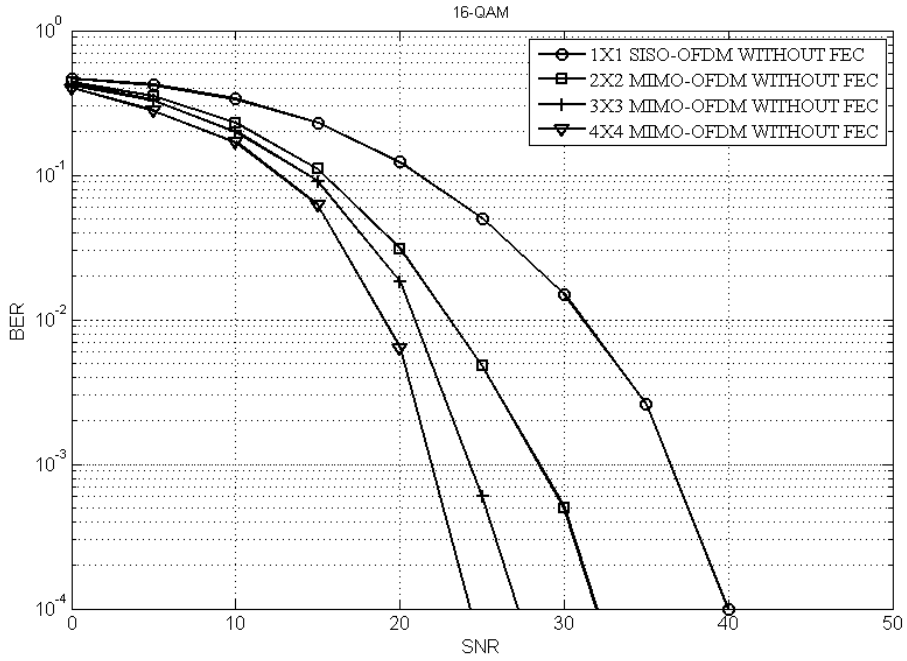

Figure 35: BER vs SNR Plots for 16QAM over Rayleigh Channel Without FECs

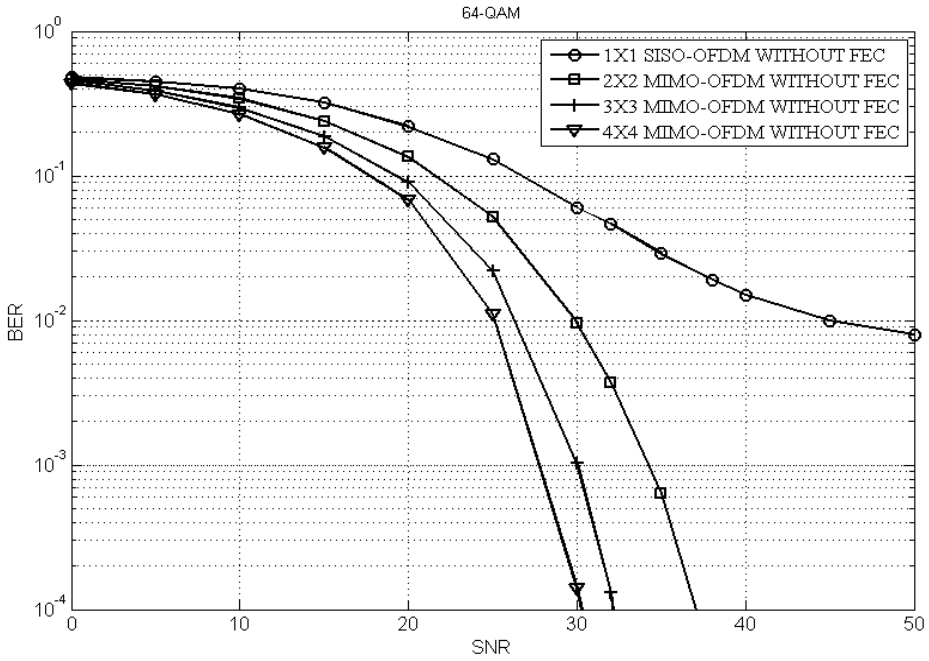

Figure 36: BER vs SNR plots for 64QAM over Rayleigh Channel Without FECs

This simulation has four cases that consider the performance in accordance with the antenna configuration. The adjustment of the configuration is mainly implemented by modeling the MIMO channel and changing the settings of the OSTBC Encoder and Combiner. The modeling of 1 × 1, 2 × 2, 3 × 3 and 4 × 4 are respectively constructed as in Figures 34, 35 and 36 for QPSK, 16-QAM and 64-QAM over the Rayleigh channel without FECs.

The results obtained using the simulation methodology are shown in the figures above. These figures show the respective performance of the BERs for different antenna configurations for the MIMO(OSTBC)-OFDM system. It is clearly observed that overall, the 4 × 4 system outperforms the other cases.

5.3.3.2 MIMO(OSTBC) - OFDM Technique over Rayleigh Fading MIMO Channel with Using FECs.

The system consists of similar blocks of the previous system with added blocks representing the channel coding algorithm. The channel coding blocks are the Reed-Solomon Encoder, the Convolutional Encoder, and the Interleaver at the transmitter, and the Reed-Solomon Decoder, the Convolutional Decoder and the Deinterleaver at the receiver.

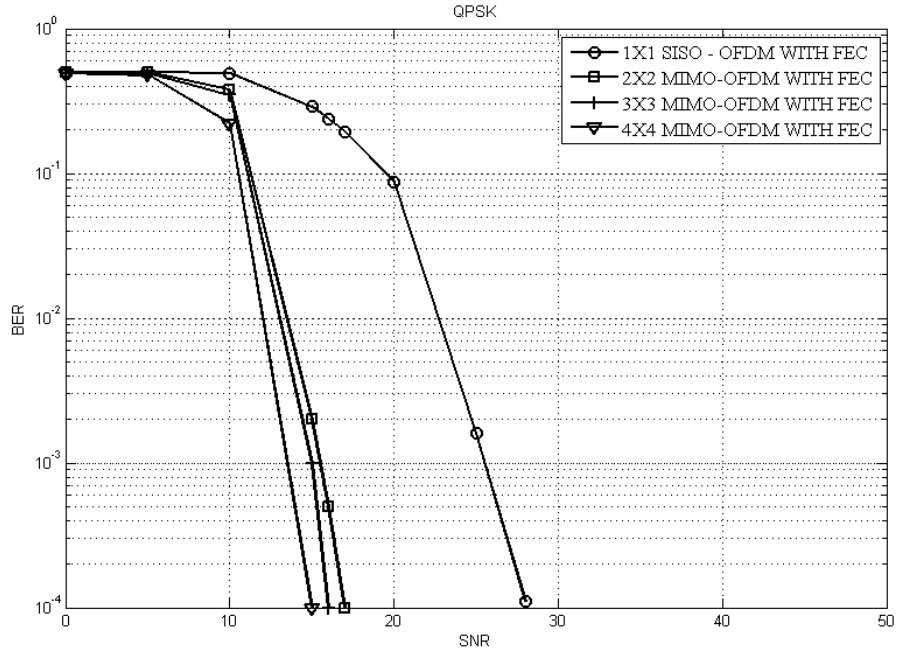

Figure 37: BER vs SNR plots for QPSK over Rayleigh channel with FECs

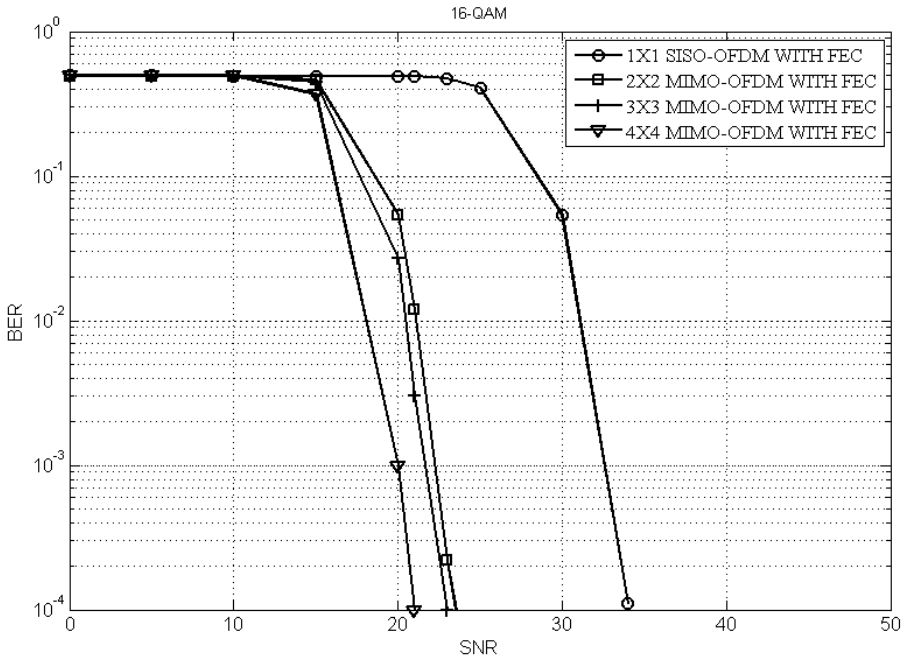

Figure 38: BER vs SNR Plots for 16QAM over Rayleigh Channel With FECs

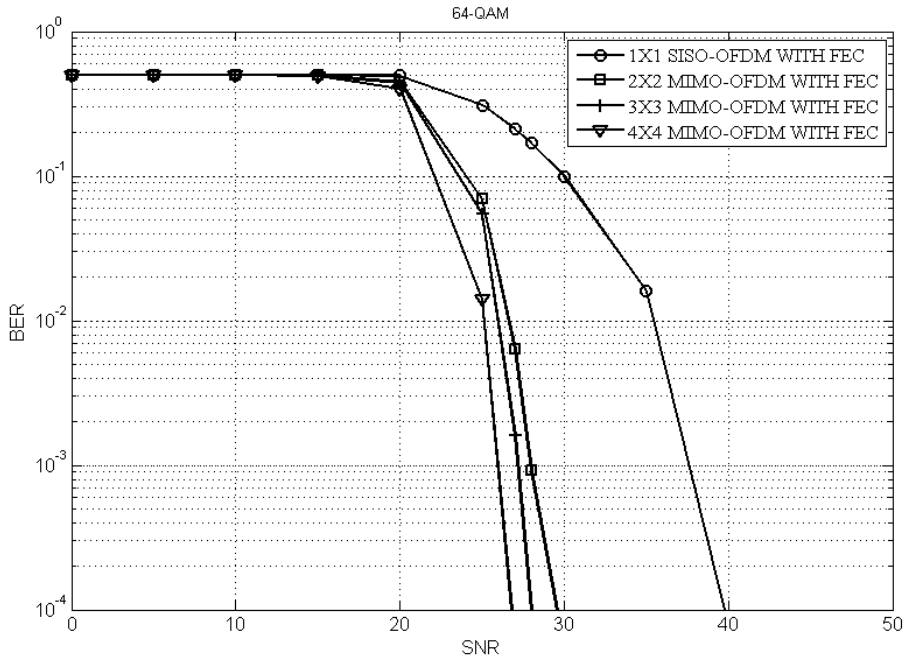

Figure 39: BER vs SNR Plots for 64QAM over Rayleigh Channel With FECs

The transmitter and the receiver are connected through a Rayleigh fading channel. The simulation results are presented in the form of BER curves over numerous values of the SNR. Figure 37 shows the variations of the BER as a function of the SNR if the modulation is QPSK and for different numbers of transmit and receive antennas with FEC over the Rayleigh channel. The bit error rate BER increases gradually for the 2×2 configuration compared to the increase in the number of antennas on the transmitter and receiver side. For the 3×3 and 4×4 antenna configuration, the BER decreases.

The BER results obtained using the simulation are presented in Figures 37, 38 and 39, which show the performance of 1×1, 2×2, 3×3 and 4×4 MIMO(OSTBC)-OFDM for QPSK, 16-QAM and 64-QAM over the Rayleigh channel with FECs. The performance of the FEC concatenated code clearly outperforms that of the same system without FECs from Figure 39. It can be seen that the FEC curve displays less flattening effect and has a much better slope than the other technique. It is clearly shown that BER with coding performs much better than BER without coding. Moreover, the MIMO(OSTBC)-OFDM system has been introduced with different antenna configurations, namely 1×1, 2×2, 3×3 and 4×4. The improvement standards using channel coding are purposed to optimize the system in terms of error decrease. From the simulation results, it was found that error reduction

performs better as the number of antennas increases. Additionally, channel coding performance is observed with significantly higher SNR values.

5.3.4 Study of Different Antenna Configurations for MIMO-OFDM using OSTBC System over Rician Fading MIMO Channel.

In this section, the performance of MIMO-OFDM using OSTBC and the Rician channel is simulated by the MATLAB program.

5.3.4.1. MIMO(OSTBC) - OFDM Technique over Rician MIMO Fading Channel without Using FECs.

In this simulation, the BER performance of SISO and MIMO wireless communication systems over the Rician channel is compared. The MIMO wireless communication system consists of 2 × 2, 3 × 3 and 4 × 4 antenna configurations. QPSK, 16-QAM and 64-QAM digital modulation schemes are exploited in each scheme. Additionally, in each scheme, the results of simulation of the BER performance of the MIMO systems are calculated.

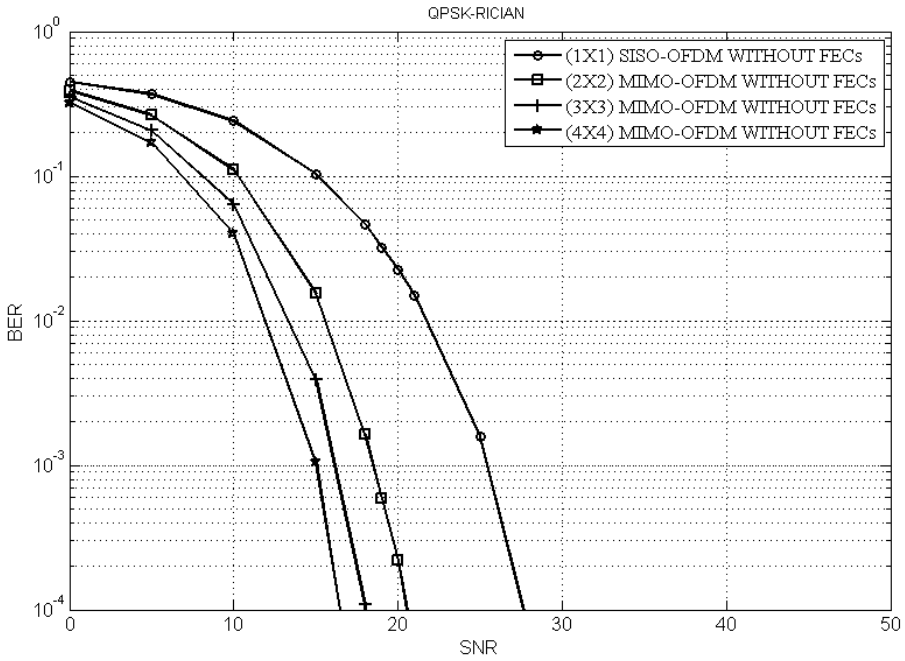

Figure 40: BER vs SNR Plots for QPSK over Rician Channel Without FECs

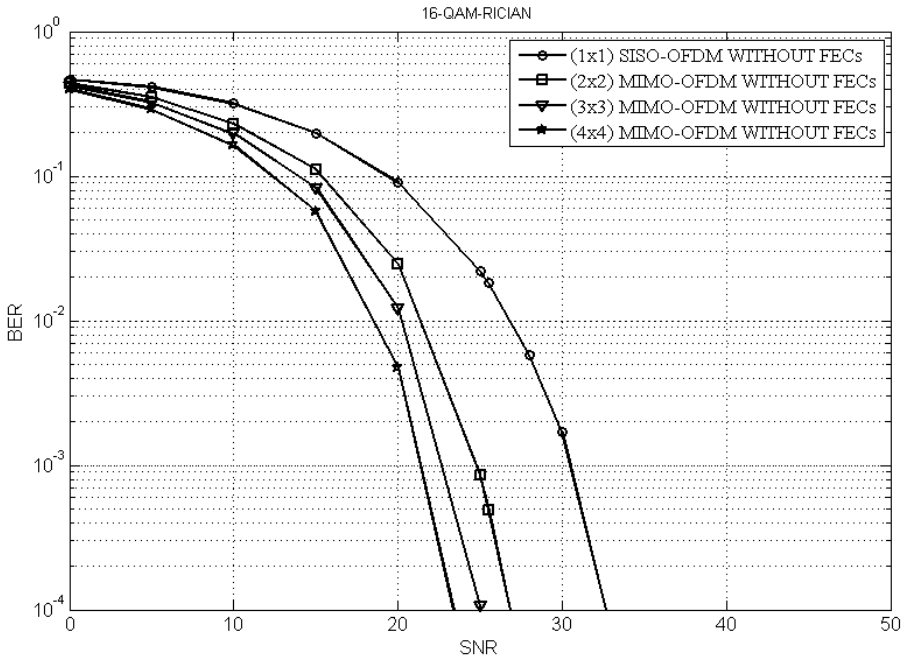

Figure 41: BER vs SNR Plots for 16-QAM over Rician Channel Without FECs

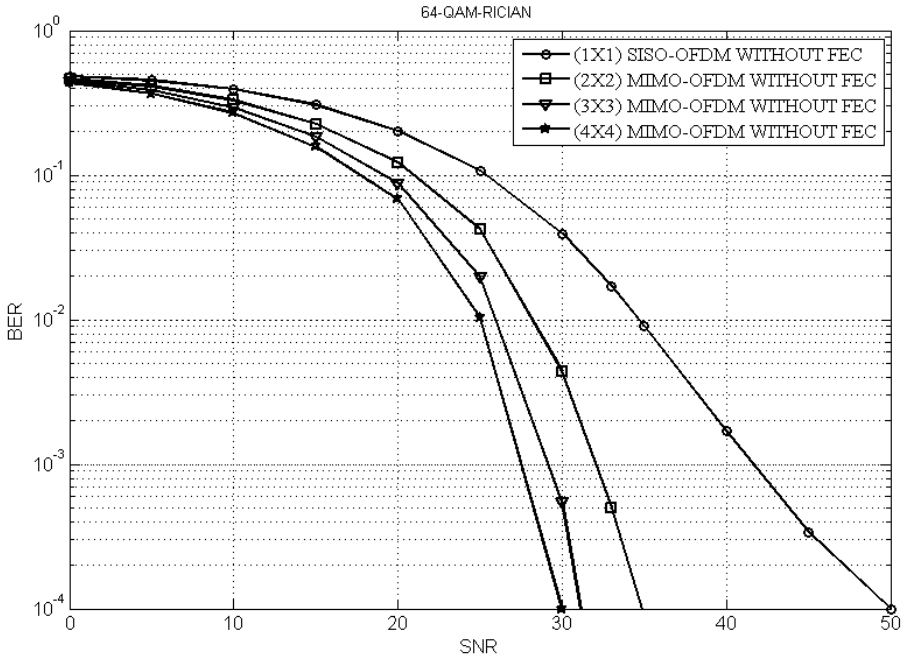

Figure 42: BER vs SNR Plots for 64-QAM over Rician Channel Without FECs

Figure 40 shows the BER performance of the system model of SISO 1 × 1 and MIMO 2 × 2, 3 × 3 and 4 × 4 over the Rician channel without FEC. Every scheme is modulated by the QPSK modulation scheme. The comparison of the BER performance confirms that MIMO 4 × 4 has the best BER performance. In contrast, the SISO 1 × 1 scheme has the worst BER performance. For example, at a 10^{-4} BER

reference, SISO needs approximately 28 dB, whereas the MIMO system with two transmit and receive antennas needs about 20.5 dB. MIMO with three receive and transmit antennas needs about 18 dB and MIMO with four transmit and receive antennas needs only about 15.5 dB.

Figure 41 shows the BER performance of the system model of SISO and MIMO with 2 × 2, 3 × 3 and 4 × 4 configurations over the Rician channel without FEC. Every scheme is modulated by the 16-QAM modulation scheme. The comparison of the BER performance confirms that MIMO 4 × 4 has the best BER performance. In contrast, the SISO 1 × 1 scheme has the worst BER performance. For example, at a 10^{-4} BER reference, SISO needs approximately 33 dB, whereas the MIMO system with two transmit and receive antennas needs about 26 dB. MIMO with three receive and transmit antennas needs about 25 dB and MIMO with four transmit and receive antennas needs only about 24 dB.

Figure 42 shows the BER performance of the SISO system model and MIMO with 2 × 2, 3 × 3 and 4 × 4 configurations over the Rician channel without FEC. Every scheme is modulated by the 64-QAM modulation scheme. The comparison of the BER performance confirms that the MIMO 4 × 4 scheme has the best BER performance. In contrast, the SISO 1 × 1 scheme has the worst BER performance. For example, at 10^{-4} BER reference, SISO needs approximately 50 dB, whereas the MIMO system with two transmit and receive antennas needs about 45 dB. MIMO with three receive and transmit antennas needs about 31.5 dB and MIMO with four transmit and receive antennas needs only about 30 dB.

5.3.4.2. MIMO(OSTBC) - OFDM Technique over Rician MIMO Fading Channel with Using FECs.

The basic idea of OFDM-MIMO is to improve the data rate and/or quality of the BER by using multiple antennas in the transmitter and receiver of the communication system with FECs over the Rician channel. The MIMO system uses Orthogonal Space Time Block Coding (OSTBC) as the core scheme.

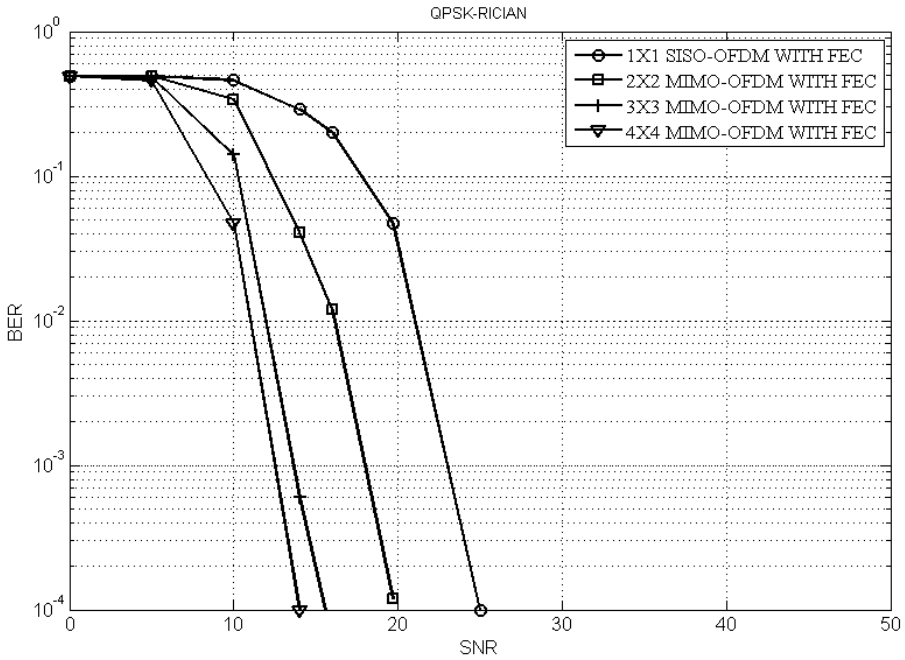

Figure 43:BER vs SNR Plots for QPSK over Rician Channel With FECs

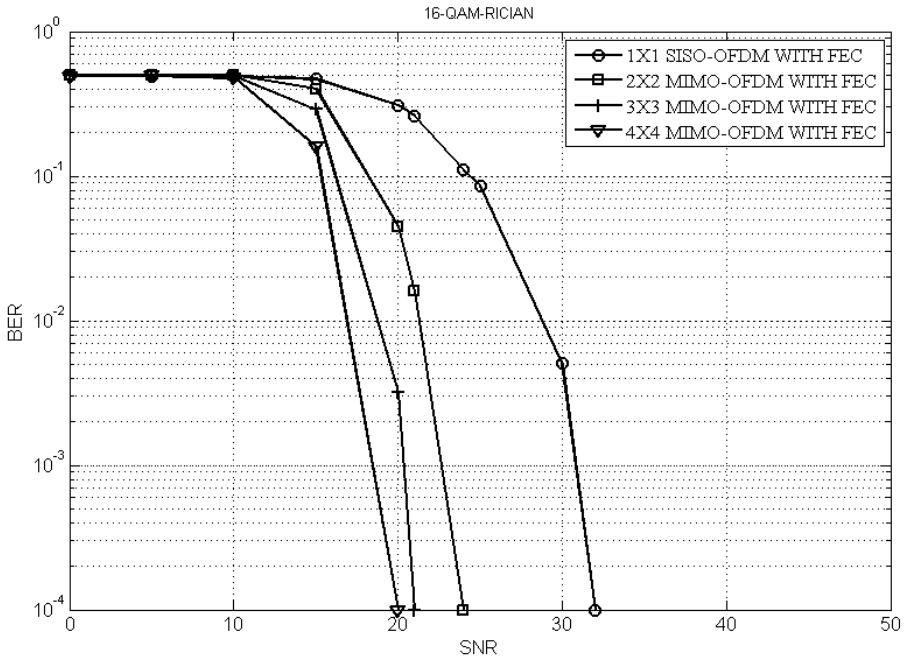

Figure 44: BER vs SNR Plots for 16-QAM over Rician Channel With FECs

Figure 43 shows how the system performs if the modulation is QPSK with FECs and for different antenna configurations with the Rayleigh channel. In general, the system performs better as we increase the number of transmissions and/or reception antennas with FECs. The SNR is equal to 25 dB for the SISO-OFDM system, 20 dB for the

2 × 2 MIMO-OFDM system, 16 dB for the 3 × 3 MIMO-OFDM system, and decreases to 13.5 dB for 4 × 4 MIMO-OFDM systems when the value of the bit error rate ratio equals 10^{-4}. When increasing the value of the SNR, we notice a significant decrease in the BER. We extracted the BER for different antenna configurations and saw that the performance for the 4 × 4 antenna configuration of the MIMO-OFDMsystem with FECs was better than the performance of all the other shown configurations.

Figure 44 shows how the system performs if the modulation is 16-QAM with FECs and for different antenna configurations with the Rayleigh channel. In general, the system performs better as we increase the number of transmissions and/or reception antennas with FECs. The SNR is equal to 32.5 dB for the SISO-OFDM system, 24.5 dB for the 2 × 2 MIMO-OFDM system, 21.5 dB for the 3 × 3 MIMO-OFDM system, and decreases to 20 dB for 4 × 4 MIMO-OFDMsystems when the value of the bit error rate ratio equals 10^{-4}. When increasing the value of the SNR, we notice a significant decrease in the BER. We extracted the BER for different antenna configurations and saw that the performance for the 4 × 4 antenna configuration of the MIMO-OFDM system with FECs was better than the performance of all the other shown configurations.

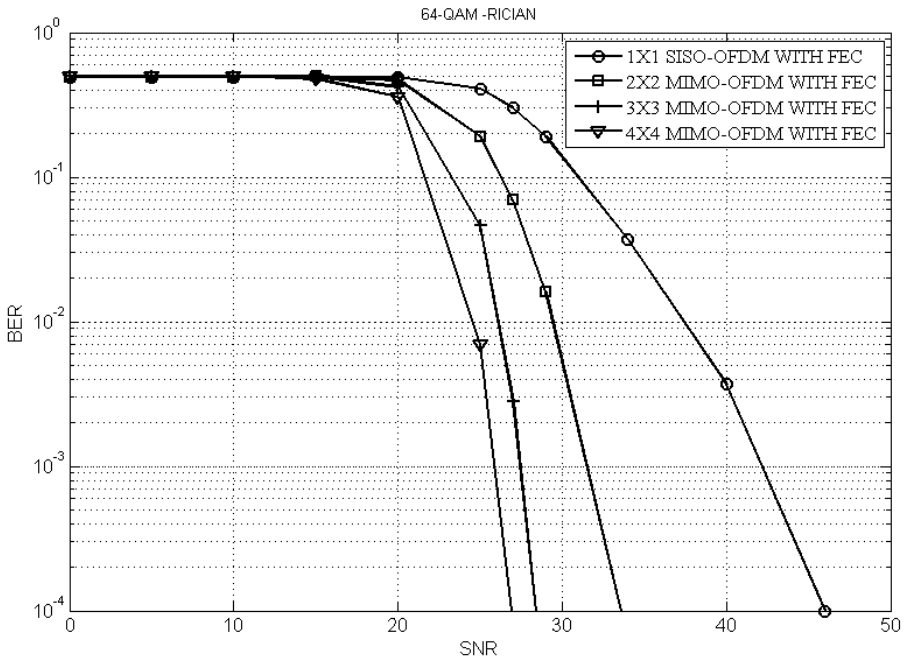

Figure 45:BER vs SNR Plots for 64-QAM over Rician Channel With FECs

Figure 45 shows how the system performs if the modulation is 64-QAM with FECs and for different antenna configurations with the Rayleigh channel. In general, the system performs better as we increase the number of transmissions and/or reception antennas with FECs. The SNR is equal to 46 dB for the SISO-OFDM system, 34.5 dB for the 2 × 2 MIMO-OFDM system, 17.5 dB for the 3 × 3 MIMO-OFDM system and decreases to 16 dB for 4 × 4 MIMO-OFDM systems when the value of the bit error rate ratio equals 10^{-4}. When increasing the value of the SNR, we notice a significant decrease in the BER. We extracted the BER for different antenna configurations and saw that the performance for the 4 × 4 antenna configuration of the MIMO-OFDM system with FECs was better than the performance of all the other shown configurations.

CHAPTER 5

Conclusion and Future Scope

5.1 Conclusion

A significant effort has been made in 5G in terms of communications with higher reliability. MIMO systems and antenna arrays are two common methods of transmitting multiple copies of data to receivers. STCs provide performance improvement in terms of lower error in multiple antenna schemes compared to single antenna schemes. STBC and STTC are the two basic forms of STBs. In STBC, the coding matrix is generated in such a manner that all the codes are orthogonal to each other and that no two codes are repeated. This orthogonal property makes the STBC scheme an OSTBC scheme and it makes the decoding of the receiver simpler. The encoded OSTBC method is used to analyze the MIMO scheme to achieve highly reliable transmission.

In this thesis, a detailed overview and analysis of OFDM-MIMO using orthogonal space-time coding was discussed. An OFDM modulator and demodulator were formed and simulated for SISO and MIMO. To remove ICI, the cyclic prefix was used with a multipath fading channel being used between the transmitter and receiver to develop simulation results. Depending on the number of transmitting antennas on the transmitting side and the number of receiving antennas on the receiver side of the system, the bit error rate (BER) simulation results for various scenarios show the significant performance gain achieved when using the OSTBC scheme with FECs.

Firstly, we implemented the MIMO-OSTBC scheme on two different channels (the Rayleigh Fading Channel and the Rician Fading Channel) using QPSK modulation and different antenna configurations. Figures 27 and 31 show that at a BER of 10^{-4}, SNR gains of 6 dB and 3 dB are achieved using a 4×4 MIMO-OSTBC without FECs over the Rayleigh fading channel and 4×4 MIMO-OSTBC with FECs over the Rayleigh fading channel, respectively. Figure 31 shows that the BER performance of

4 × 4 transmit diversity OSTBC data transmission over the Rician Fading Channel with FECs for a 4 × 4 antenna configuration at a BER of 10^{-4} results in SNR gains of 4.5 dB. It can be seen from the simulation results that better BER performance can be obtained with the use of more antennas due to the fact that multiple antenna systems achieve better performance than single antenna systems. We have come to the conclusion that the system with FECs can be more effective.

Secondly we implemented MIMO-OFDM schemes using OSTBC and FECs. The proposed RC-CC with the interleaving model was carried out under three modulation schemes, namely QPSK, 16-QAM, and 64-QAM under two-channel models, and the Rayleigh and Rician for four antenna configurations, namely 1 × 1, 2 × 2, 3 × 3 and 4 × 4. MIMO-OFDM under the Rayleigh fading channel with FECs for QPSK and a 4 × 4 antenna configuration show that at a BER of 10^{-4}, SNR gains of 14 dB are achieved. Figures 40 and 43 show that at a BER of 10^{-4}, SNR gains of 17 dB and 13.5 dB are achieved using 4 × 4 MIMO-OFDM without FECs over the Rician fading channel and 4 × 4 MIMO-OFDM with FECs over the Rician fading channel, respectively. The QPSK modulation scheme has better performance in comparison to 16-QAM and 64-QAM in both channels.

Finally, as the number of transmitters and receivers increases, the BER performance of the system also increases. However, with acceptable FEC BER, more advanced technology is needed to observe other forward error corrections, which is considered future work.

REFERENCES

[1] **Pratt T., Walkenhorst B., Nguyen S., (2009),** "Adaptive polarization transmission of OFDM signals in channels with polarization mode dispersion and polarization-dependent loss". IEEE Transactions on Wireless Communications, vol.8, no.7, pp.3354-3359.

[2] **Drakshayini N. and Singh A. V., (2016),** "An Efficient Orthogonal Frequency Division Multiplexing (OFDM) System and Performance Analysis of Digital Audio Broadcasting (DAB) System". International Journal of Computer Applications, vol.148, no.8.

[3] **Wang S., Li C., Wang K., (2005),** "A multi-band multi-standard RF front-end IEEE 802.16 a for IEEE 802.16 a and IEEE 802.11 a/b/g applications". In 2005 IEEE International Symposium on Circuits and Systems , pp. 3974-3977.

[4] **Fernandes B. and Sarmento H., (2012),** "FPGA implementation and testing of a 128 FFT for a MB-OFDM receiver". Analog Integrated Circuits and Signal Processing, vol.70, no.2, pp. 241-248.

[5] **Cho, S., Kim, J., YangY., Kang, G., (2010),** "MIMO-OFDM wireless communications with MATLAB". John Wiley & Sons.

[6] **Tarokh V., Jafarkhani H., Calderbank, R., (1999),** "Space-time block codes from orthogonal designs". IEEE Transactions on Information theory, vol.45, no.5, pp. 456-1467.

[7] **Ganesan G. and Stoica P., (2001),** "Space-time block codes: A maximum SNR approach". IEEE Transactions on Information Theory, vol.47, no.4, pp. 1650-1656.

[8] **Wolniansky W., Foschini J., GoldenD., Valenzuela A., (1998),** "V-BLAST: An architecture for realizing very high data rates over the rich-scattering wireless channel". In 1998 URSI international symposium on signals, systems, and electronics. Conference proceedings (Cat. No. 98EX167), pp. 295-300.

[9] **Ha J., Mody N., Sung H., Barry R., McLaughlin W., Stüber L., (2002),** "LDPC coded OFDM with Alamouti/SVD diversity technique". Wireless Personal Communications, vol.23, no.1, pp. 183-194.

[10] **Jiang M. and Hanzo L., (2007).** "Multiuser MIMO-OFDM for next-generation wireless systems". Proceedings of the IEEE, vol.95, no.7, pp.1430-1469.

[11] **Tu C. C. and Champagne B., (2008),** "Subspace blind MIMO-OFDM channel estimation with short averaging periods: Performance analysis". In 2008 IEEE Wireless Communications and Networking Conference , pp. 24-29.

[12] **Tarighat A. and Sayed A. H., (2005),** "MIMO OFDM receivers for systems with IQ imbalances". IEEE Transactions on Signal Processing, vol.53, no.9, pp. 3583-3596.

[13] **Deshmukh S. and Bhosle U., (2018),** "Analysis of OFDM-MIMO with BPSK Modulation and Different Antenna Configurations Using Alamouti STBC". In Optical and Wireless Technologies . Springer, Singapore. , pp. 1-9.

[14] **Agarwal A. and Mehta S. N., (2018),** "Development of MIMO–OFDM system and forward error correction techniques since 2000s". Photonic Network Communications, vol.35, no.1, pp. 65-78.

[15] **Sawarkar S. and Dutta S., (2016),** "Performance Analysis of BER Using Efficient Coding and Interleaving Techniques in MIMO-OFDM System". International Journal of Computer Science and Network, vol.5, no.1, pp. 78-83.

[16] **Pandey A. and Sharma S., (2014),** "BER performance of OFDM system in AWGN and Rayleigh fading channel". International Journal of Engineering Trends and Technology (IJETT), vol.13.

[17] **Chaudhari N., Vishwakarma D., Patel B., (2013),** "BER Improvement in MIMO system using OFDM". International Journal of Advanced Research in Computer Science and Electronics Engineering (IJARCSEE), vol.2, no.1, pp. 019.

[18] **O'hara B. and Petrick A., (2005),** "IEEE 802.11 handbook: a designer's companion". IEEE Standards Association.

[19] **Andrews G., Ghosh A., Muhamed, R., (2007),** "Fundamentals of WiMAX: understanding broadband wireless networking". Pearson Education.

[20] **Hanzo L., Akhtman Y., Akhtman, J., Wang L., Jiang M., (2011),** "MIMO-OFDM for LTE, WiFi and WiMAX: Coherent versus non-coherent and cooperative turbo transceivers". John Wiley & Sons.

[21] **Nuaymi L., (2007),** "WiMAX: technology for broadband wireless access". John Wiley & Sons.

[22] **Wang L. and Jezek B., (2008),** "OFDM modulation schemes for military satellite communications". In MILCOM 2008-2008 IEEE Military Communications Conference, pp. 1-7.

[23] **Khalid F. and Speidel J., (2010),** "Advances in MIMO techniques for mobile communications-a survey". Int'l J. of Communications, Network and System

Sciences, vol.3 no. 03, pp.213.

[24] **Wannstrom J., (2013),** "LTE-advanced. Third Generation Partnership Project (3GPP) ".

[25] **Tran T., Shin Y., Shin S., (2012),** "Overview of enabling technologies for 3GPP LTE-advanced". EURASIP Journal on Wireless Communications and Networking, vol.2012 no. 1, pp.54.

[26] **Nee V. and Prasad R., (2000),** "OFDM for wireless multimedia communications". Artech House, Inc..

[27] **Bracewell R. N. and Bracewell R. N., (1986),** "The Fourier transform and its applications". New York: McGraw-Hill.

[28] **Galli S., Koga H., Kodama N., (2008),** "Advanced signal processing for PLCs: Wavelet-OFDM". In 2008 IEEE International Symposium on Power Line Communications and Its Applications , pp. 187-192.

[29] **Li Y. G. and Stuber G. L., (2006),** "Orthogonal frequency division multiplexing for wireless communications". Springer Science & Business Media.

[30] **Hanzo L., Münster M., Choi B., Keller T., (2005),** "OFDM and MC-CDMA for broadband multi-user communications, WLANs and broadcasting". John Wiley & Sons.

[31] **LaSorte N., Barnes J., Refai H., (2008),** "The history of orthogonal frequency division multiplexing". In IEEE GLOBECOM 2008-2008 IEEE Global Telecommunications Conference , pp. 1-5.

[32] **Weinstein S. and Ebert P., (1971),** "Data transmission by frequency-division multiplexing using the discrete Fourier transform". IEEE transactions on Communication Technology, vol.19 no. 5, pp. 628-634.

[33] **Li B., Qin Y., Low P., Gwee L., (2007),** "A survey on mobile WiMAX [wireless broadband access]". IEEE Communications magazine, vol.45 no. 12, pp. 70-75.

[34] Ahmadi S., (2010), "Mobile WiMAX: A systems approach to understanding IEEE 802.16 m radio access technology". Academic Press.

[35] **Li Q., Lin E., Zhang J., Roh, W., (2009),** "Advancement of MIMO technology in WiMAX: from IEEE 802.16 d/e/j to 802.16 m". IEEE Communications Magazine, vol.47 no. 6, pp. 100-107.

[36] **Witrisal K., (2004),** "Basics of OFDM and Synchronization". In OFDM for Wireless Communications Systems, Artech House , pp. 117-148.

[37] **Kim I., Han Y., Chung K., (2010),** "An efficient synchronization signal structure for OFDM-based cellular systems". IEEE Transactions on Wireless Communications, vol.9 no. 1 , pp. 99-105.

[38] **Jain M., and Roja, M. M., (2005),** "Comparison of OFDM with CDMA System in Wireless Telecommunication for multipath delay spread". In 2005 1st IEEE and IFIP International Conference in Central Asia on Internet , pp. 1-5.

[39] **Matiae D., (1998),** "OFDM as a possible modulation technique for multimedia applications in the range of mm waves". Introduction to OFDM, vol.1, pp.10-30.

[40] **Sadat A., and Mikhael W. B., (2001),** "Fast Fourier Transform for high speed OFDM wireless multimedia system". In Proceedings of the 44th IEEE 2001 Midwest Symposium on Circuits and Systems. MWSCAS 2001 (Cat. No. 01CH37257) , vol.2, pp. 938-942.

[41] **Lei S. W. and Lau V. K., (2002),** "Performance analysis of adaptive interleaving for OFDM systems". IEEE transactions on Vehicular Technology, vol.51 no. 3, pp. 435-444.

[42] **Murch R. D. and Letaief K. B., (2002),** "Antenna systems for broadband wireless access". IEEE Communications Magazine, vol.40 no. 4, pp. 76-83.

[43] **Rappaport T. S., (1996),** "Wireless communications: principles and practice , vol. 2 ". New Jersey: prentice hall PTR.

[44] **Papoulis A. and Pillai S. U., (2002),** "Probability, random variables, and stochastic processes". Tata McGraw-Hill Education.

[45] **Correia L. M., (2010),** "Mobile broadband multimedia networks: techniques, models and tools for 4G". Elsevier.

[46] **Zhang W., Xia G., Letaief B., (2007),** "Space-time/frequency coding for MIMO-OFDM in next generation broadband wireless systems". IEEE Wireless Communications, vol.14 no. 3, pp. 32-43.

[47] **Kashima T., Fukawa K., Suzuki H., (2006),** "Adaptive MAP receiver via the EM algorithm and message passings for MIMO-OFDM mobile communications". IEEE Journal on Selected Areas in Communications, vol.24 no. 3, pp. 437-447.

[48] **Paulraj J., Gore A., Nabar U., Bolcskei H., (2004),** "An overview of MIMO communications-a key to gigabit wireless". Proceedings of the IEEE, vol.92 no. 2, pp. 198-218.

[49] **Shin, C., Heath W., Powers J., (2007),** "Blind channel estimation for MIMO-OFDM systems". IEEE Transactions on Vehicular Technology, vol.52 no. 2,

pp. 670-685.

[50] **Rosenhouse I. and Weiss A. J., (2007),** "Combined analog and digital error-correcting codes for analog information sources". IEEE transactions on communications, vol.55 no. 11, pp. 2073-2083.

[51] **Bolcskei H., (2006),** "MIMO-OFDM wireless systems: basics, perspectives, and challenges". IEEE wireless communications, vol.13 no. 4, pp. 31-37.

[52] **Alamouti S. M., (1998),** "A simple transmit diversity technique for wireless communications". IEEE Journal on selected areas in communications, vol.16 no. 8 , pp. 1451-1458.

[53] **Shah H., Hedayat A., Nosratinia A., (2006),** "Performance of concatenated channel codes and orthogonal space-time block codes". IEEE transactions on wireless communications, vol.5 no. 6, pp. 1406-1414.

[54] **Loskot P. and Beaulieu N. C., (2009),** "Approximate performance analysis of coded OSTBC-OFDM systems over arbitrary correlated generalized Ricean fading channels". IEEE transactions on communications, vol.57 no. 8, pp. 2235-2238.

[55] **Gupta B. and Saini D. S., (2012),** "A low complexity decoding scheme of STFBC MIMO-OFDM system". In 2012 Wireless Advanced (WiAd) , pp. 176-180.

[56] **Daniels C., Caramanis M., Heath W., (2009),** "Adaptation in convolutionally coded MIMO-OFDM wireless systems through supervised learning and SNR ordering". IEEE Transactions on vehicular Technology, vol.59 no. 1, pp. 114-126.

[57] **Khan M. N. and Ghauri S., (2008),** "The WiMAX 802.16 e physical layer model".

[58] **Marks R., (2003),** "IEEE Standard 802.16 for global broadband wireless access". In ITU Telecom World 2003 Forum.

[59] **Wicker S. B., (1995),** "Error control systems for digital communication and storage (Vol. 1) ". Englewood Cliffs: Prentice hall.

[60] **Berlekamp E. R., (1968),** "Algebraic coding theory McGraw-Hill". New York.

[61] **Rao K. D., (2015),** "Channel coding techniques for wireless communications". Springer India.

[62] **Van Zelst A. and Schenk T. C., (2004),** "Implementation of a MIMO OFDM-based wireless LAN system". IEEE Transactions on signal processing, vol. 52 no. 2, pp. 483-494.

[63] **Alausta G. M., (2020),** "Comparative Study of Different Antenna Configurations for the MIMO-OSTBC Technique Using FEC and the Rayleigh Fading Channel". Recent Advances in Electrical & Electronic Engineering (Formerly Recent Patents on Electrical & Electronic Engineering), vol. 13 no. 7, pp. 1022-1027.